Pathway simulations in common oncogenic drivers of leukemic and rhabdomyosarcoma cells: A systems biology approach

GEORGE I. LAMBROU[1], APOSTOLOS ZARAVINOS[2], MARIA ADAMAKI[1], DEMETRIOS A. SPANDIDOS[2], FOTINI TZORTZATOU-STATHOPOULOU[1] and SPIROS VLACHOPOULOS[1]

[1]First Department of Pediatrics, Choremeio Research Laboratory, University of Athens, Athens 11527; [2]Laboratory of Virology, Medical School, University of Crete, Heraklion 71110, Crete, Greece

Received December 19, 2011; Accepted February 6, 2012

DOI: 10.3892/ijo.2012.1361

Abstract. A part of current research has intensively been focused on the proliferation and metabolic processes governing biological systems. Since the advent of high throughput methodologies such as microarrays, the load of genomic data has increased geometrically and along with that the need for computational methods to interpret these data. In the present study, we investigated *in vitro* the common proliferation and metabolic processes, associated with common oncogenic pathways, as far as gene expression is concerned, between the T-cell acute lymphoblastic leukemia (CCRF-CEM) and the rhabdomyosarcoma (TE-671) cell lines. We present a computational approach, using cDNA microarrays, in order to identify commonalities between diverse biological systems. Our analysis predicted that JAK1, STAT1, PIAS2 and CDK4 are the driving forces in the two cell lines. This type of analysis may lead to the understanding of the common mechanisms that transform physiological cells to malignant, and may reveal a new holistic approach to understanding the dynamics of tumor onset as well as the mechanistics behind oncogenic drivers.

Introduction

It is a fact that tumors can be as diverse as the patients carrying them. Due to these differences, tumors are extremely difficult to cure, as the effects of treatments differ depending on the patient. Previously, Nicolis showed that stem cells are found in different tumor types, suggesting that they can be the etiology of tumor maintenance and growth (1). However, there is evidence that even normal, already differentiated cells can be transformed into tumorigenic ones (1). Perilongo *et al* also reported a case of a child manifesting five different tumor types simultaneously (2). It may be possible that stem cells originating from the same organism possess similar mutations or alterations, thus giving rise to five different tumor types. Therefore, there is a need for the investigation of common pathways between different tumor types. The discovery of similar or opposite gene expression profiles could lead us to the understanding of a common tumor origin, if such exists.

A number of studies have investigated the detection of cancer germ line genes (CGGs) both in pediatric sarcomas (3) and pediatric brain tumors (4). The discovery of global antigens for tumor vaccines could become salvatory for childhood malignancies (3). Other studies have reported the common appearance of antigens in Ewing's sarcoma/primitive neuroectodermal tumor (EWS/PNET) with lymphoblastic lymphoma (5). Rhabdomyosarcoma (RMS) belongs to the PNET family of tumors, which utilize embryonic genes for their progression (6). Acute lymphoblastic leukemia (ALL), which originates from the lymphoblast, also uses embryonic mechanisms for its differentiation and progression.

Another point which requires attention is the regulation of genes through transcription factors (TFs). Knowledge of gene regulatory networks is considered to be of crucial importance for understanding diseases such as cancer, and may lead to new therapeutic approaches (7). Furthermore, the knowledge of common transcription regulatory networks could be of critical importance, as it could lead to a universal treatment for a diverse disease, such as cancer.

At the same time, there is much debate accompanying the advent of the next-generation sequencing technologies, concerning the role of mutations in the oncogenic pathways. Previous reports have stressed this issue mentioning that, on the one hand, the presence of mutations is a prerequisite for tumorigenesis, and on the other hand, some of these mutations are required for the appearance of neoplasias (8-12). In particular, in the studies by Parsons *et al* (13) and Pleasance *et al* (8) there is an effort to link the detection of mutations with gene expression in the tumor samples. At this point, we could add that the existence of one or more mutations, is probably not the adequate causative effect for the formation of a tumor, due to the fact that the existence of mutations *per se*, means nothing if the mechanism does not support them.

Correspondence to: Dr George I. Lambrou, First Department of Pediatrics, Choremeio Research Laboratory, University of Athens, Goudi 11527, Athens, Greece
E-mail: glamprou@med.uoa.gr

Key words: T-cell acute lymphoblastic leukemia, CCRF-CEM cell line, rhabdomyosarcoma, TE-671 cell line, flow cytometry, microarrays, chromosome mapping, transcription factor binding motif analysis, Gene Ontology, pathway analysis, physical protein-protein interactions prediction

ALL is the most frequently occurring tumor among childhood malignancies. It originates from the undifferentiated lymphoblast whose development is blocked at different stages on its way to becoming the mature lymphoid cell, thus giving rise to a tumor. Acute leukemia emerges mainly during childhood although it can also occur in adolescents, manifesting a poorer prognosis in this age group. RMS is also a rare childhood cancer comprising 5-8% of all tumors emerging during childhood. The cell of origin is considered to be the myoblast or cells that will form the skeletal muscle. These cells differ from the smooth cells that line the intestinal tract. Theoretically, RMS can emerge in any part of the body that has skeletal muscle; however, it originates mainly in the head and neck. Thus, these two malignancies are of different origin. The common aspect between these malignancies is that they both comprise of cells that are undifferentiated, immortal and potentially divide infinitely. Also, looking back to their developmental history, both cell types originate from the embryonic mesoderm. Myoblasts originate from the dorsal (paraxial) mesoderm, whereas blood cells are derived from the lateral mesoderm which gives rise to the splanchnic mesoderm, which in turn gives rise to hemangioblastic tissue. Blood cells originate from two sites in embryogenesis: The first is considered to be the ventral mesoderm near the yolk sac, whereas hematopoietic cells that last the lifetime of an organism are derived from the mesodermal area surrounding the aorta. From this point, differentiation enables these two cell types to have different functions and roles in the body, through differential gene regulation.

Of note, it has been reported that RMS can be present in the bone marrow of patients presenting a leukemic image, without the presence of a primary tumor (14-17). It has also been reported that the presentation of a secondary malignancy after successful treatment of the primary tumor, is possible. Such a case was reported by Kaplinsky *et al* who showed that the successful treatment of a paravertebral embryonal RMS (ERS) resulted in the development of T-cell acute lymphoblastic leukemia (T-ALL) (18). Our query was whether the development of the secondary tumor could be the cause of cells originating from the primary tumor, due to therapy-related leukemia, or whether it could be due to the presence of leukemic cells, which after being in a dormant state in the bone marrow, were triggered after chemotherapy of the RMS. The first case implies that the same tumor cell possesses two traits: The ability to migrate and differentiate into another cell type, thus manifesting stem cell-like properties. This reinforces the stem cell theory of the origin of cancer, as cancer stem cells keep the ability to differentiate, migrate and grow into a new malignancy, with almost completely new traits.

However, it is also known that therapy-related leukemia can occur due to the use of chemotherapeutics (19,20). This phenomenon has not been thoroughly investigated and the mechanisms behind it still remain obscure. However, it points out to the fact that carcinogenesis is a complicated phenomenon, which includes a plethora of cell fate mechanisms as opposed to single events. Due to the complexity of its nature, there is currently a need for the use of computational methods in the study of carcinogenesis. Moreover, if the hypothesis of the simultaneous presence of two different tumor cells in different locations is true, this would suggest that stem cells play a major role in carcinogenesis and tumor growth. On the other hand, an interesting report by Kelly *et al* showed that, at least in part, the presence of cancer stem cells is not necessary for tumor growth (21).

The present study is concerned with the common expressional profile of two cell lines: The T-ALL (CCRF-CEM) and the RMS (TE-671) cell lines. Our investigation focused on the identification of genes that share a common expression profile between the two cell lines. Both cell lines are characterized by the fact that their differentiation has stopped at an early stage, before they mature to their final cell type. Normally, these cells would have matured and progressed into differentiated cells, constituting blood and muscle cells, respectively. At some unknown point, normal differentiation ceased for these cells and they became malignant. From that point on, to the first manifestation of symptoms of malignancy, there is a lack of knowledge regarding the mechanisms underlying oncogenesis.

From these observations, the question arises of whether two distinct cell types destined to fulfill different functions, manifest similar mechanisms of growth and progression due to their malignant character. The present study focused on the identification of the differential expression profiles underlying the two cell lines. A previous report studied the expression profile of seven ARMS cell lines possessing the PAX3-FKHR fusion gene, along with other cell lines of different tumor types (22). To our knowledge, this is the first report comparing two completely different types of neoplasia, such as the CCRF-CEM and TE-671 cell lines. These mechanisms are examined with the purpose of identifying common drivers that lead to the progression of tumor cells. We hereby propose a new computational approach for the investigation of common oncogenic drivers.

Materials and methods

Cell cultures. The CCRF-CEM (ALL) and the TE-671 (RMS) cell lines were used as the model, both obtained from the European Collection of Cell Cultures (ECACC). The CCRF-CEM cell line, a $CD4^+$ (23) and $CD34^+$ presenting cell line (24), was initially obtained from the peripheral blood of a two-year-old Caucasian female. The tumor was diagnosed as lymphosarcoma which later progressed to acute leukemia (25). The child had undergone irradiation therapy and chemotherapy prior to obtaining the cell line. Although remission was achieved at various stages, the disease progressed rapidly (25). The cell line has been observed to undergo minor changes after long-term culture, except for the presence of dense granules in the nucleoli (26). Finally, the CCRF-CEM cell line has been reported to manifest autocrine catalase activity which participates in its mechanisms of growth and progression (27).

The TE-671 cell line was initially reported to have been obtained from a cerebellar medulloblastoma of a six-year old Caucasian female, prior to irradiation therapy (28), and characterized later on (29). However, it is currently known that this cell line is parental if not identical to the RD (30) RMS cell line. However, a number of reports still refer to this cell line as medulloblastoma (31,32).

Both cell lines were seeded at the -24 h time-point and allowed to grow overnight. After 24 h (time, 0 h) a sample was taken from both cell lines in order to perform measurements

and every 24 h thereafter. CCRF-CEM cells were grown in RPMI-1640 medium supplemented with 2 mM L-glutamine and 100 U/ml streptomycin/penicillin (Gibco), 20% FBS (Gibco) at 37˚C, 5% CO_2 and ~100% humidity. TE-671 cells were grown in DMEM (Gibco) medium supplemented with 2 mM L-glutamine, 10% FBS and 100 U/ml streptomycin/penicillin. Cells were allowed to grow to ~1.500x10^3 cells/μl for CCRF-CEM and at ~80% confluence for TE-671. Cells were harvested at confluence using 0.1% trypsin (only for TE-671) and centrifugation at 1000 rpm for 10 min. The supernatant was discarded and the cells were washed with pre-warmed 1X PBS, re-centrifuged at 1000 rpm for 10 min and the pellet was kept for further processing.

Cell proliferation. Cell population counts were determined with the use of a Nihon Kohden CellTaq-α hematology analyzer. Cells were counted at the -24-h time-point as well as at 0, 4, 24, 48 and 72 h after being allowed to grow under normal conditions. For this purpose, 200 μl of cell suspensions were obtained from each flask and counted directly with the analyzer.

Flow cytometry. Flow cytometry was performed on a FlowCount XL flow cytometer (Beckman Coulter, Brea, CA, USA). Cell cycle distribution and DNA content was determined with standard PI staining (Invitrogen Inc., Grand Island, NY, USA). Briefly, 1 ml of cell suspension from each flask was centrifuged at 1000 rpm for 10 min. The supernatant was removed and cells were suspended in 1 ml 75% ethyl alcohol. The cells were incubated at 4˚C overnight. After incubation, cells were centrifuged at 1000 rpm for 10 min. The supernatant was removed and cells were washed with 1 ml ice-cold PBS, pH 7.4. Cells were re-centrifuged and re-diluted in 1 ml PBS pH 7.4. RNase A (0.25 μg/ml) was added and cells were incubated at 37˚C for 30 min in order to remove any remaining traces of RNA that could interfere with PI staining. PI was added to a final concentration of 1 μg/ml. All experiments were performed in triplicate. The reported data constitute the average of three independent experiments.

Flow cytometry data analysis. Flow cytometry and cell cycle data were analyzed with WinMDI software version 2.8 (The Scripps Research Institute, Flow Cytometry Core Facility) and Cylchred version 1.0.2 (Cardiff University, Wales) which is based on the algorithms proposed by Ormerod *et al* and Watson *et al* (33-35).

RNA isolation. RNA was isolated with TRIzol reagent (Invitrogen Inc.) according to the manufacturer's instructions. The amount of RNA isolated was measured with a SmartSpec 3000 spectrophotometer (BioRad, Berkley, CA, USA) and RNA integrity was estimated by 2% agarose gel electrophoresis. At least 40 μg of RNA from each sample was used. DNase treatment (RQ1 DNAse; Promega, Fitchburg, WI, USA) followed, as described by the manufacturer. Finally, RNA samples were further purified using the RNeasy mini kit (Qiagen, Hilden, Germany) and RNA amounts and integrity were determined again as above. Samples with a 1.8 to 2.0 A_{260}/A_{280} ratio were selected. In addition, those that empirically showed a twice as bright 28S band compared to the 18S band on the gel were utilized.

Microarray experimentation. For the assay of mRNA levels two sets of microarray chips were used: cDNA microarray chips (4.8 k genes) obtained from Takara (IntelliGene™ II Human CHIP 1) (36) and microarray chips (9.6 k genes) from the Institute for Molecular Biology and Tumor Research, Microarray Core Facility of the Philipps University, Marburg, Germany (IMT9.6 k). Hybridization was performed with the CyScribe Post-Labeling kit [GE Healthcare (former Amersham Inc.), Buckinghamshire, UK] as described by the manufacturer. The fluorescent dyes used were Cy3 and Cy5. The RNA extracted from the CCRF-CEM cells was stained with Cy3 (reference) and RNA from the TE-671 cell line with Cy5 (experiment). cDNAs were purified with Qiagen PCR product clean-up kit. Slides were activated at 55˚C for 30 min in 1% BSA. Samples were applied on the slides, and allowed to hybridize overnight at 55˚C. The following day, slides were washed in 200 ml 0.1X SSC and 0.1% SDS for 3x5 min, in 200 ml 0.1X SSC for 2x5 min and in 200 ml ddH_2O for 30 sec. Slides were dried by centrifugation at 1500 rpm for 3 min and scanned with a ScanArray 4000XL microarray scanner [Perkin-Elmer Inc. (former GSI Lumonics), Waltham, MA, USA]. Images were generated with ScanArray microarray acquisition software (Perkin-Elmer Inc.). The microarray data have been submitted to the GEO Database (Accession No. GSE34522).

Microarray data analysis

Data collection. Microarray data pre-processing analysis was performed with ImaGene® v.6.0 Software (BioDiscovery Inc., El Segundo, CA, USA) and Armada software (National Hellenic Research Foundation, Athens, Greece) (37). Data were collected from exported text file and data pre-processing was performed using Microsoft Excel®. Data were processed in two ways: The first included the separation of each channel (Cy3 and Cy5), and the second included pre-processing of the ratio between the two samples.

Data pre-processing and background correction. A common pre-processing stage was applied to the raw data (the median intensity value in each channel) of both platforms. Specifically, the well performing version of the robust loess-based background correction (rLsBC) approach, as proposed by Sifakis *et al* was applied (38). rLsBC assumes that the background noise affects the spot intensities in a multiplicative manner (39). Instead of using the measurements of the local (feature-related) background for the correction, rLsBC utilizes the regression estimate of the logarithmic background distribution $B^{R,G}$ according to the logarithmic foreground intensity $F^{R,G}$ for each channel (R, red and G, green). Thus, rLsBC provides a robust estimation of the channel-specific background noise, utilized to background-correct the logarithmic foreground intensities: $F_c^{R,G} = F^{R,G} - B_l^{R,G}$ where $F_c^{R,G}$ is the logarithmic background-corrected foreground intensity, and $B_l^{R,G}$ the robust estimate of background noise, for each channel. The absolute background-corrected foreground intensity $f_c^{R,G}$ for each channel was then calculated as: $f_c^{R,G} = 2^{F_c^{R,G}}$

Normalization. The background-corrected signal intensities were further normalized in order to mitigate the effect of extraneous, non-biological variation in the measured gene expression levels. Normalization was performed by using six different methods: i) No further processing after background correction,

ii) $\log_2$ transformation, iii) lowess normalization, iv) division with the global median (median of the 50% percentile), v) subtraction of global median (the median of the 50% percentile) and vi) rank invariant with running median. Finally, the rank invariant normalization method was chosen for further processing and analysis (40-42). The rank invariant normalization approach included the robust version of the intensity-dependent scatter-plot smoother loess (43) with a quadratic polynomial model, and a smoothing parameter equal to 10%, which was considered appropriate for the relatively small number of probes attached in the microarrays. The normalization results are presented in Fig. 1. Box plots were used to examine normalization efficiency as presented in Fig. 1D.

Data integration. We performed data integration at a lower level as previously described (44). Specifically, the pre-processed datasets of each array were combined into one unified dataset, in which standard statistical procedures were applied. Nonetheless, whenever applicable to the nature of the present study, certain key issues had to be addressed, such as pre-processing, preparation and annotation of the individual datasets, in compliance with previously reported guidelines (45). In order to perform data integration, two main issues had to be resolved: i) Matching reporters on the two microarray platforms, and ii) normalizing data to address platform-related differences (46). Specifically, each reporter-level identifier (GenBank accession numbers) was mapped to a UniGene identifier (UniGene Cluster ID) (47-51). The mapping was performed through the Source web-based tool (52), simultaneously for both platforms, in order to avoid inconsistencies (53). All mapped reporter-level identifiers had a one-to-one relationship with the gene-level identifiers, that is, each reporter was associated with a single UniGene identifier and no more than one reporter was mapped to the same UniGene identifier. Reporters having insufficient information to be mapped to any gene-level identifier were omitted. Thus, a fully updated set of unique gene-level identifiers was generated for each platform.

Filtering. As low signal intensity measurements are less reliable in terms of the impact of noise on them than high gene expression measurements, an intensity-dependent filtering (54,55) with an absolute threshold value of 10 was used in each channel, in order to exclude low quality features. In addition, signal-to-noise ratio was used as:

$$SNR = \frac{\mu_{R,G} - \mu_B}{\sigma_B}$$

where $\mu_{R,G}$ and μ_B is the mean value intensity for the respective channel (Cy3 or Cy5) and mean background intensity, respectively; and σ_B is the background mean signal standard deviation. A threshold of 2 was set as a cut-off value, meaning that spot intensity for at least one channel should be twice as much as that of the background.

Analysis. The data were further analyzed in order to identify the differentially expressed genes (DEGs) and the groups of genes that share common expression characteristics. Analysis steps were conducted in the Matlab® computing environment.

Identification of DEGs. Furthermore, each gene was tested for its significance in differential expression using a z-test. Genes were considered to be significantly differentially expressed if they obtained a p-value <0.05. The false discovery rate (FDR) was calculated as previously described (56-58). There was a FDR of 1% for p<0.05 for the IntelliGene microarray chip, and a FDR of 9% for p<0.01 for the IMT 9.6 k microarray chip. Calculating the FDR for the combination of both platforms gives a FDR of 6% for p<0.01. The DEGs per experiment were identified at a confidence level of 95%.

Chromosome mapping. Chromosome mapping was performed with Genesis 1.7.2 software (Technische Universitaet-Graz, Austria) using Pearson's correlation, Spearman's rank order correlation (59-61) and the WebGestalt web-tool (Vanderbilt University, The Netherlands; http://bioinfo.vanderbilt.edu/gotm/) (62).

Transcription factor binding motif (TFBMs) analysis. TFBMs were searched in the Transcription Element Listening System Database (TELiS) (www.telis.ucla.edu) (63) and WebGestalt web-tool (Vanderbilt University; http://bioinfo.vanderbilt.edu/gotm/) (62). The TRANSFAC TF database was used for the identification of gene TF binding sites (64).

Gene Ontology (GO) analysis. GO analysis was performed using the eGOn online tool for Gene Ontology (The Norwegian University of Science and Technology, Trondheim, Norway, http://www.genetools.microarray.ntnu.no/egon/) (65), Genesis 1.7.2 software (60) and the WebGestalt web-tool (62). Correlations between the DEGs and the TFBMs were further investigated using the PubGene Ontology Database (www.pubgene.org). For literature search the Microarray Literature-based Annotation (MILANO) (http://milano.md.huji.ac.il/; Department of Molecular Biology, Hadassah Medical School, Hebrew University, Jerusalem, Israel) web-based tool was utilized (66). Gene definitions and functions were based on the National Institutes of Health databases (http://www.ncbi.nlm.nih.gov/sites/entrez/).

Pathway analysis. The DEGs were mapped on different pathways using Pathway Explorer software (Technical University of Graz, Austria) (67). The percentage of genes that were present in all known pathways was investigated, using the databases available through the Pathway Explorer software. The KEGG database of pathways was used for our analysis (68-72), as well as CellDesigner (73,74) and Matlab v.7.6.0 computation environment with SimBiology®. For the analysis of merged pathways the KEGGConverter Tool was utilized (National Hellenic Research Foundation, Athens Greece, http://www.grissom.gr/keggconverter) (75).

Results

Cell proliferation, morphology and cell cycle. Cells were allowed to grow under normal conditions for a total of 96 h (from -24 to 72 h) until they reached a final population of ~$1.5x10^3$ cells/μl. Cells were harvested and processed further for cell cycle distribution. As expected, cells manifested different forward vs. side scatter (FS vs. SS) distributions (Fig. 2C and D). CCRF-CEM cells manifested a more homogeneous population compared to TE-671 cells. TE-671 cells

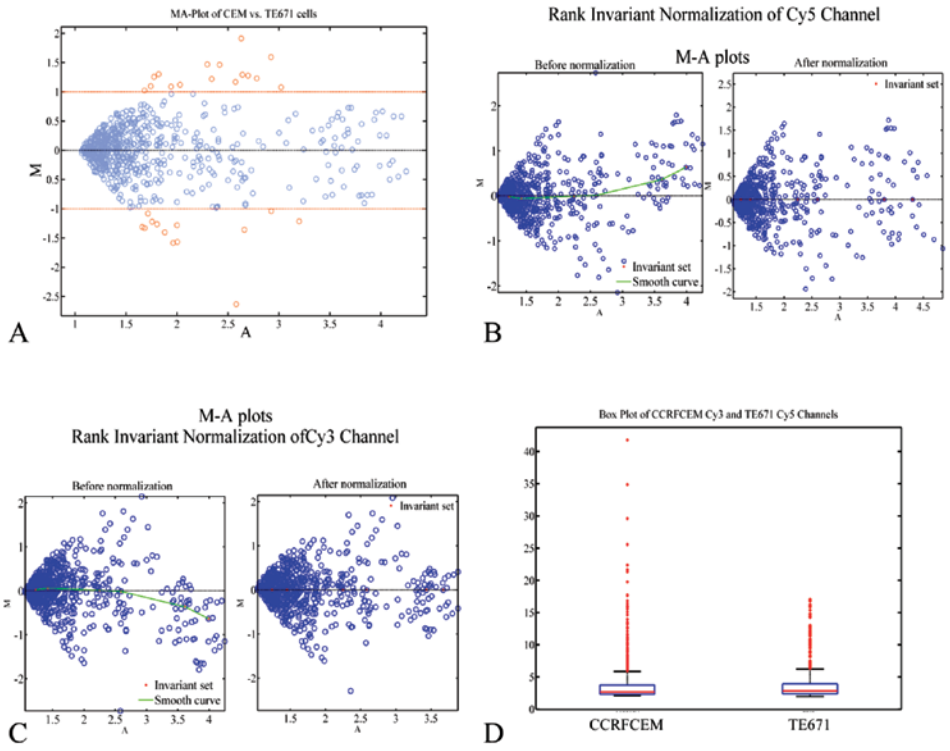

Figure 1. Microarray data normalization. (A) MA plot with robust loess normalization. Rank invariant normalization for the (B) Cy5 and (C) Cy3 channels. (D) A box-plot of the two channels manifests that normalization has eliminated the bias between the two samples.

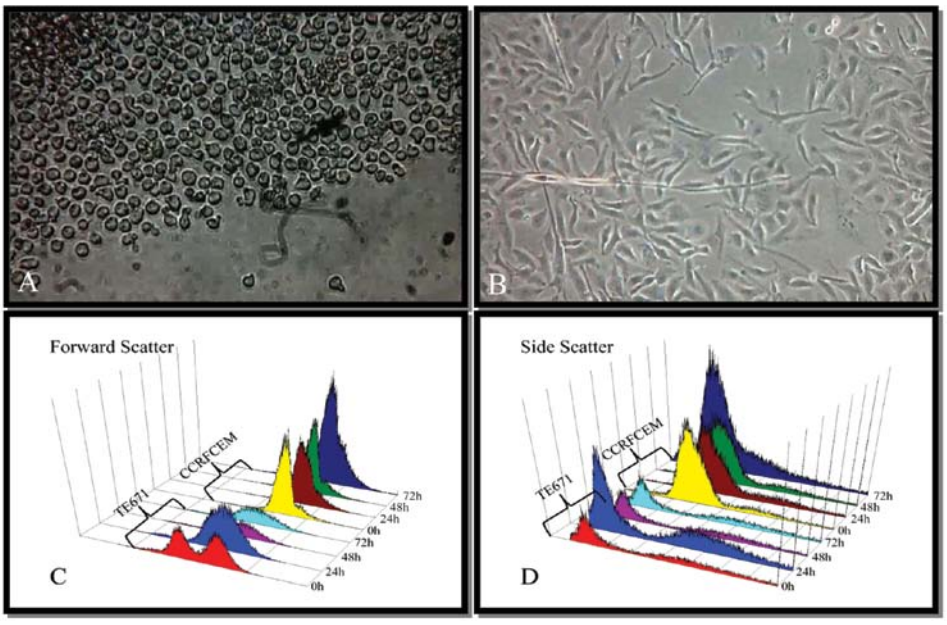

Figure 2. Morphology of the (A) CCRF-CEM and (B) TE-671 cell lines as presented by microscopy. Flow cytometry using the (C) forward scatter plot and (D) side scatter plot.

manifested a cell population with greater variance both for size and granularity. This was expected since CCRF-CEM cells grow in suspension (Fig. 2A) which gives more uniformity to their morphology, whereas TE-671 cells are adherent (Fig. 2B) and when trypsinized, they produce a cell population with a different morphology. Cell cycle distribution showed a different pattern of growth. CCRF-CEM cells entered the S-phase rapidly after 24 h in culture (from -24 to 0 h) and displayed cycling behavior thereafter (Fig. 3A). This indicated that the cell cycle for this type of cell is rapid, since the interchange between the phases progressed rapidly. The TE-671 cells entered the S-phase with a slower decrease in G1-phase changes and a relatively small change in G2-phase (Fig. 3B). No significant differences were observed in the G2-phase

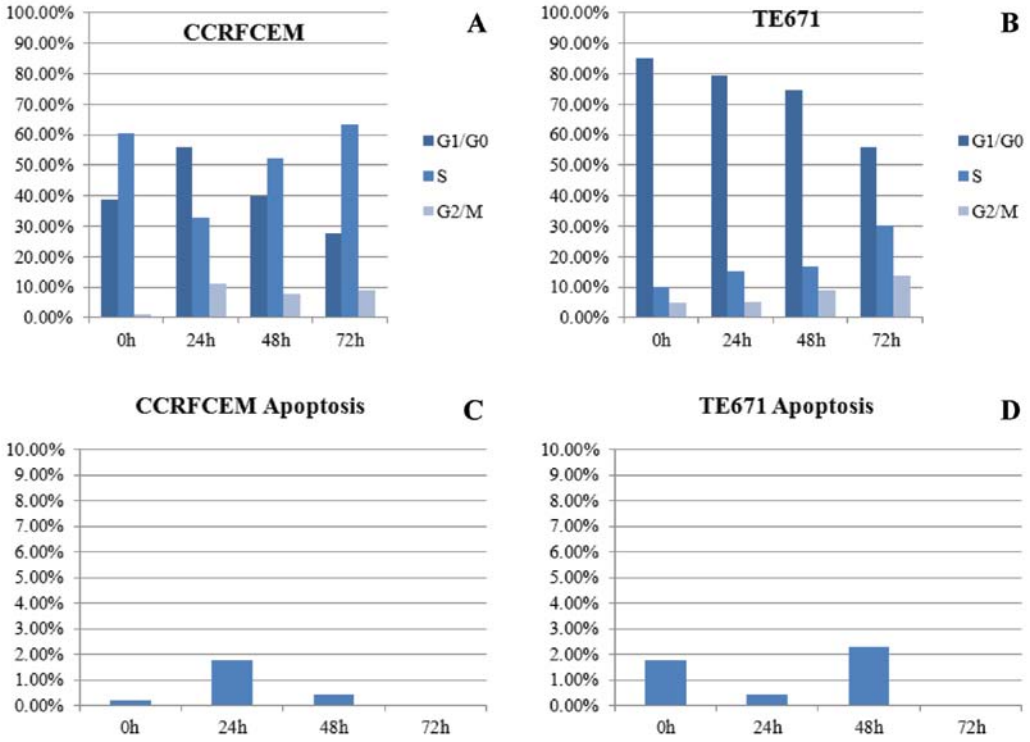

Figure 3. Cell cycle distribution with respect to time for the (A) CCRF-CEM and (B) TE-671 cell lines. Apoptosis was very low for the (C) CCRF-CEM and (D) TE671 cell lines.

between the two cell lines. Although both cell lines enter the cell cycle phases in different percentages, they follow the same growth pattern, indicating a common pattern of reaction to environmental stimuli, in this case spatial-temporal growth. This growth pattern was expected to be reflected on the gene expression profile at 72 h. In addition, apoptosis measured as the fraction of cells with DNA fragmentation for the CCRF-CEM (Fig. 3C) and the TE671 cells (Fig. 3D) showed very low levels indicating that cells were proliferating under ideal conditions.

Microarrays. At 72 h the cells were harvested and further processed for microarray analysis. As mentioned in Materials and methods we analyzed our data in two ways: First, we separated the two channels and compared the intensities of each gene within the same cell type; and second, we considered the ratio of the two samples and analyzed them, respectively. DEGs were identified using the z-test, and genes with a p-value <0.05 were considered significant. All other genes were considered to be equally expressed. Microarray analysis of the Takara and IMT platforms showed a total of 660 and 45 genes, respectively (including ESTs) i.e., good quality spots showing the three main types of expression (over-, under- and unchanged expression). In total, from the revealed genes, 228 are reported to be related to leukemia, 78 to RMS, 76 to the CCRF-CEM cell line and eight to the TE-671 cell line. Fig. 4 presents the DEGs acquired by each type of analysis. The significantly expressed genes in both samples, as well as in the comparison between them, were AF143888, AK025762, BTBD3, CYP39A1, KCTD3, NM_016130, NPFF and UBFD1. All these genes were down-regulated in the TE-671 cells, compared to the CCRF-CEM cells (Fig. 4C). These genes are possibly the ones that are unique to each cell type and are what differentiates the two cell types from each other. In Table I we summarize the list of the DEGs.

Chromosome mapping. Genes were mapped on the 24 human chromosomes. Chromosome mappings included: i) All genes after filtering for each channel separately, ii) ratio of samples for all genes after filtering, iii) common DEGs for each channel separately, iv) DEGs for the ratio of samples, v) common non-significant genes for each channel separately and to the ratio of samples.

All genes after filtering for each channel separately. There was a relatively equivalent distribution of DEGs on each chromosome, with an exception of chromosome 1, on which 71 genes (10.66%) were mapped. Chromosome 2 contained 48 DEGs (7.21%), followed by chromosome 6 with 36 DEGs (5.4%), and chromosomes 4 and 10 with 31 and 25 DEGs, respectively (~4.7%). On chromosomes 3, 5, 11, 12, 15 and 19 ~25 DEGs (~4%) were mapped. The X chromosome contained 31 DEGs (3.7%) (Fig. 5). One interesting observation was that the number of genes did not correlate with the levels of expression on each chromosome. Thus, the highest levels of expression were observed on chromosomes 12, 18 and 19 and not on chromosomes 1 and 2, which had the largest number of genes mapped.

Ratio of samples for all genes after filtering. The mean gene expression was estimated for the ratios of Cy5 over Cy3 (Fig. 6). The highest average expression was noticed on chromosome 14.

Common DEGs for each channel separately. The separation of the DEGs based on their chromosomal expression is

Table I. Significantly expressed genes in each channel (Cy3 and Cy5) as well as within the ratio TE-671/CCRF-CEM.

Gene	CCRF-CEM_Cy3_pval	Intensity	Gene	TE-671_Cy5_pval	Intensity	Gene	CCRF-CEM vs. TE-671
CYP39A1	7.1181E-18	41.78389	**IL2RA**	1.1722E-06	19.8	**AF143888**	-1.11181989
NPFF	2.06086E-12	34.88156	**FEM1B**	1.87947E-06	16.05107	**AK025762**	-1.060984567
TIMP4	2.06086E-12	34.88156	**ZZEF1**	5.12501E-06	13.49114	**AP1M2**	-2.18484153
UBFD1	5.71072E-09	29.62511	**NT5C2**	8.51751E-06	9.22704	**ARNTL**	1.091262573
AF143888	1.00031E-06	25.55424	**FBXL3**	1.01757E-05	8.089721	**BTBD3**	-1.142440024
AP1M2	3.21699E-05	22.35297	**PDCD5**	2.16887E-05	8.873451	**C2**	-1.290484292
DLC1	3.21699E-05	22.35297	**YARS**	5.35643E-05	16.05107	**CCDC53**	-1.038802341
ZHX3	3.21699E-05	22.35297	**HTR2B**	5.92953E-05	8.480922	**CEP110**	1.025893175
BTBD3	3.21699E-05	22.35297	**AF143323**	5.92953E-05	17.7375	**CSNK2A2**	-2.139800134
AK025762	6.28664E-05	21.67371	**SETD4**	9.67539E-05	8.394905	**CTGF**	-1.089390928
KCTD3	8.58147E-05	21.34997	**LOC151146**	0.00012813	13.49114	**CXCL11**	1.016058683
FNDC5	0.000354065	19.8	**ZHX3**	0.00073264	22.35297	**CYP39A1**	-1.707316518
FAM149B1	0.000354065	19.8	**CYP39A1**	0.000985502	41.78389	**DACH1**	-1.24508579
IL2RA	0.000354065	19.8	**TEAD3**	0.00101255	10.69104	**FRMD4A**	-2.206263944
NM_016130	0.000354065	19.8	**FNDC5**	0.001045795	19.8	**GCHFR**	1.126350953
CSNK2A2	0.001940284	17.7375	**ELF2**	0.00113142	10.3248	**GRB10**	1.301414043
AF143323	0.001940284	17.7375	**NPFF**	0.001395187	34.88156	**HCCS**	1.225409758
AF339813	0.001940284	17.7375	**WDR73**	0.001994343	9.299133	**HPS5**	1.375196388
REG1B	0.00206522	17.65667	**DLC1**	0.002682338	22.35297	**IQSEC3**	1.607186666
WNT5A	0.003774239	16.85313	**UBFD1**	0.002682338	29.62511	**KCTD3**	-1.176427672
C2	0.00518102	16.41317	**ST8SIA5**	0.002798241	13.96587	**KIAA1576**	-1.423011109
CAMKK2	0.006677182	16.05107	**AK023784**	0.003175562	8.229248	**MAPK10**	1.42649399
FEM1B	0.006677182	16.05107	**AF143888**	0.003312011	25.55424	**NM_016130**	-1.053562688
FRMD4A	0.006677182	16.05107	**CXorf1**	0.003352045	12.71281	**NM_033330**	-1.681687739
YARS	0.006677182	16.05107	**CDKN2AIP**	0.003836985	7.582367	**NPFF**	-1.47748396
PRC1	0.007626474	15.85763	**AF339813**	0.004262618	17.7375	**NTRK3**	-1.630961081
HEATR5A	0.009286442	15.56609	**IFNG**	0.00474939	10.94917	**PIP4K2A**	1.139230626
DACH1	0.012670831	15.09318	**ZFP112**	0.005613631	9.07462	**PNPLA4**	1.308630477
SPRED2	0.016721875	14.65653	**RAB1A**	0.005782065	2.301637	**PTEN**	-1.875701466
ST8SIA5	0.025456793	13.96587	**CAMKK2**	0.009469924	16.05107	**RAB11A**	-1.108030918
PLEKHG1	0.026325184	13.90909	**PLEKHG1**	0.010509901	13.90909	**RAB1A**	2.300999087
LOC151146	0.033541148	13.49114	**PHACTR1**	0.010548857	10.13494	**RLF**	-1.183184819
ZZEF1	0.033541148	13.49114	**ZDHHC13**	0.010906781	8.082386	**SHBG**	-1.399176198
NM_001174	0.038312596	13.25541	**WNT5A**	0.011061282	16.85313	**SPCS2**	1.242593156
WDR82	0.038379272	13.2523	**WDR35**	0.011685815	6.237717	**TIMP4**	-3.215464573
NM_033330	0.039661634	13.19332	**PRC1**	0.012011647	15.85763	**TNFAIP3**	-1.129228828
			ADORA1	0.012201291	12.50751	**TPD52L2**	1.537979298
			ARHGEF7	0.015813135	7.076865	**UBFD1**	-1.303757805
			AK025762	0.016007345	21.67371	**WSB2**	1.046956075
			NM_001174	0.016007345	13.25541	**ZNF184**	-1.133300923
			NAV3	0.017381377	11.20593		
			SPRED2	0.020097086	14.65653		
			BTBD3	0.020771574	22.35297		
			FAM149B1	0.024638426	19.8		
			C15orf23	0.027589911	11.52492		
			IKZF5	0.027751518	12.07221		
			NM_016130	0.036060401	19.8		
			HEATR5A	0.03756187	15.56609		
			KCTD3	0.039205175	21.34997		
			REG1B	0.040634735	17.65667		
			WDR82	0.040927424	13.2523		

All genes are indicated by bold letters.

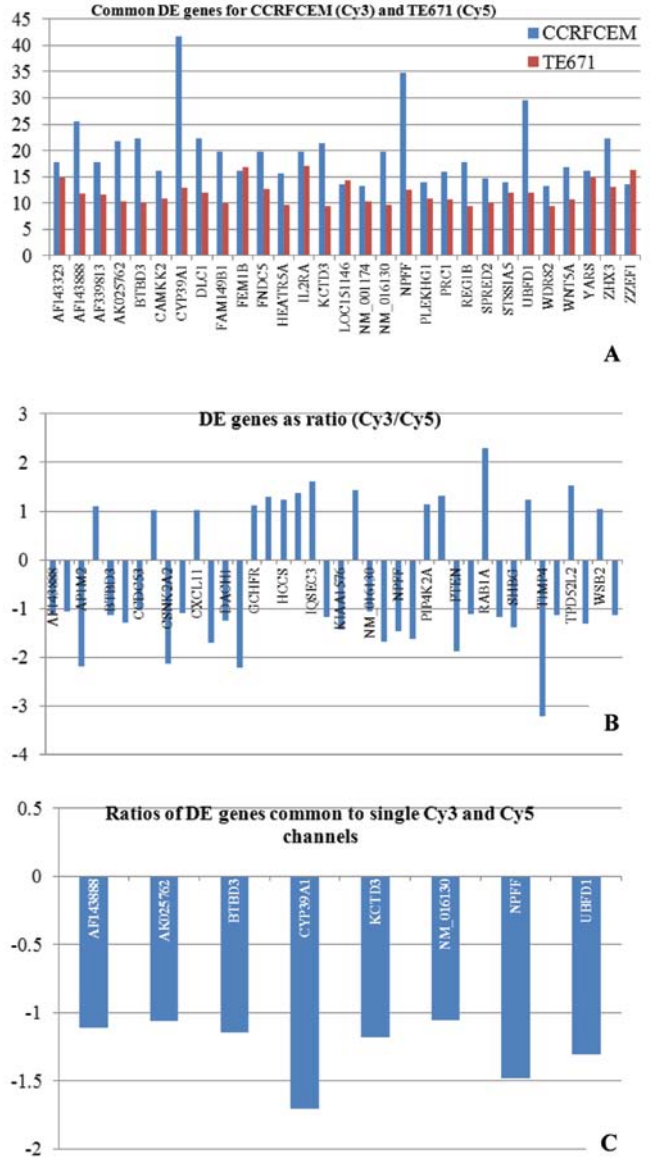

Figure 4. Microarray data of (A) each channel, (B) of gene ratios and (C) common DEGs both to individual channels and ratios. DE, differentially expessed.

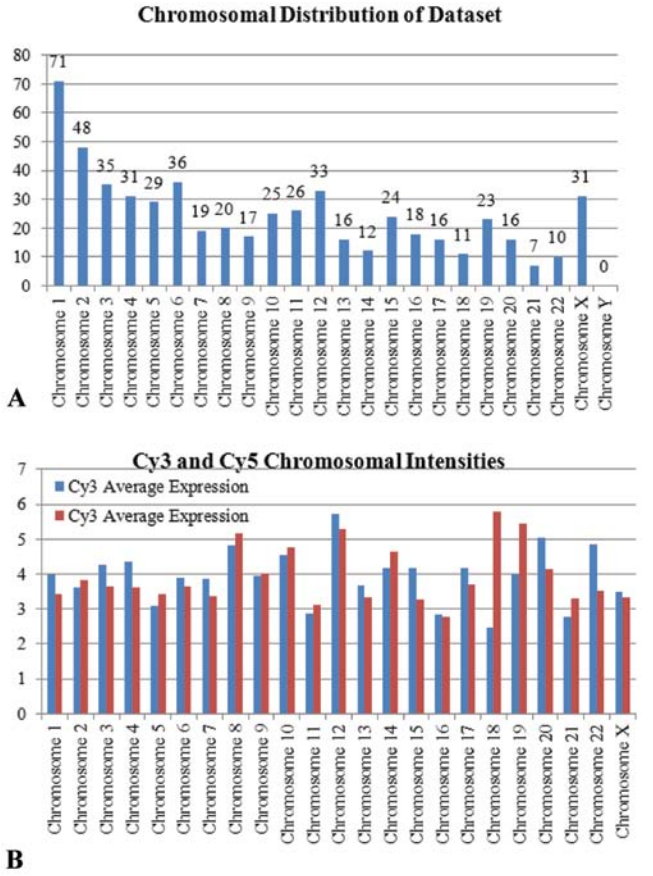

Figure 5. (A) Chromosomal expression of all genes, and (B) separately for each channel (Cy3 and Cy5).

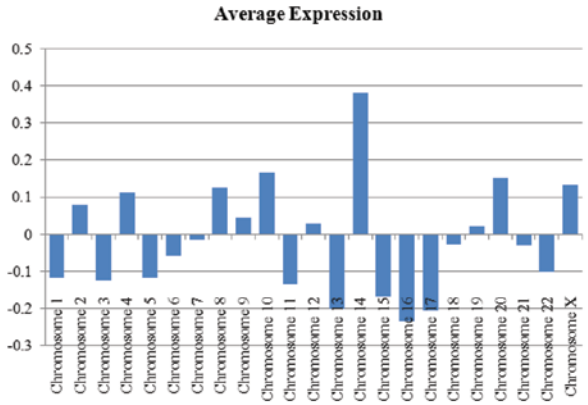

Figure 6. Chromosome-based average gene expression of the ratio Cy5/Cy3.

presented in Fig. 7. Highest levels of expression were observed on chromosomes 6 and 16.

DEGs for the ratio of samples. The DEGs were also explored with respect to the ratio between the two samples (Fig. 8).

Common non-significant genes for each channel separately and to the ratio of samples. Finally, we explored the chromosomal distribution of the common non-significant genes, since they are commonly expressed in both cells. The results are presented in Fig. 9.

Correlation between gene numbers and gene expression. Our observation after analyzing the chromosome-based intensities was that the gene number per chromosome was irrelevant to the gene expression levels. This led us to the assumption that there may be a correlation pattern between chromosomes, genes and expression levels. Therefore, we attempted to perform fitting and simulation procedures in our data, in order to find such patterns. Curve fittings did not give significant results (Fig. 10A-D). A possible reason for this is that chromosome expression on the one hand should follow some basic dynamics rules, but on the other hand it is of non-linear nature; therefore, it cannot be fitted with linear equations. Continuing with this analysis, 3D surface fittings produced some interesting results, as it appeared that the average gene expression either as single intensities or ratios, was fitted with polynomial and loess approximations with a R^2>0.9 and root mean square error (RMSE) of <0.4 (Fig. 10E-H).

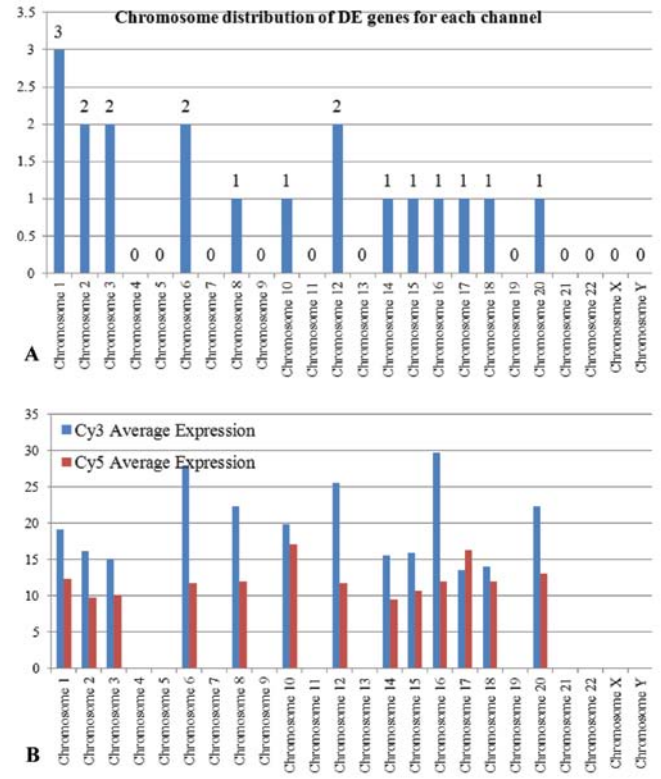

Figure 7. (A) Chromosome distribution and (B) expression of the DEGs, separately for each channel (Cy3 and Cy5). DE, differentially expessed.

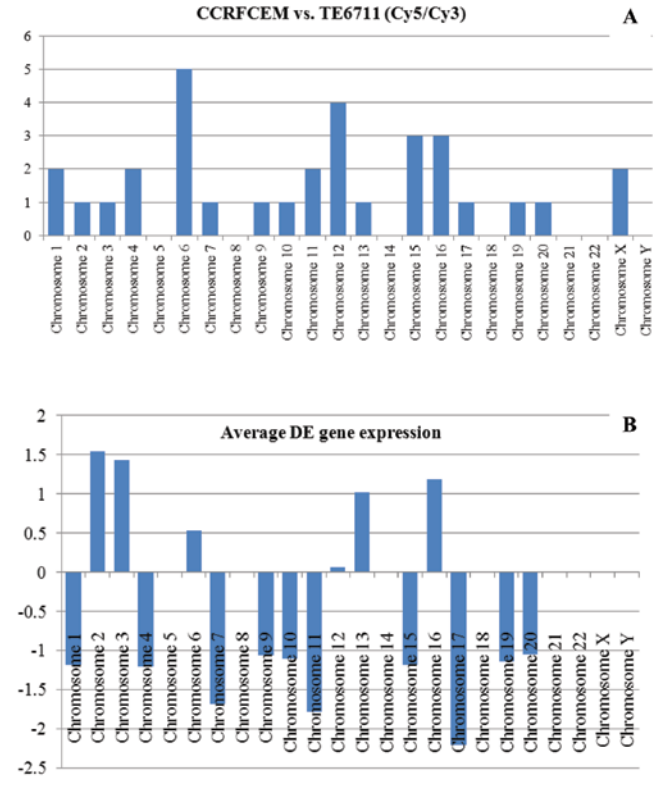

Figure 8. Chromosomal gene expression of the (A) DEGs and (B) average gene expression of the ratio Cy5/Cy3. DE, differentially expessed.

TFBMs. TFBM analysis was performed with the common DEGs between those significant for each channel and the gene

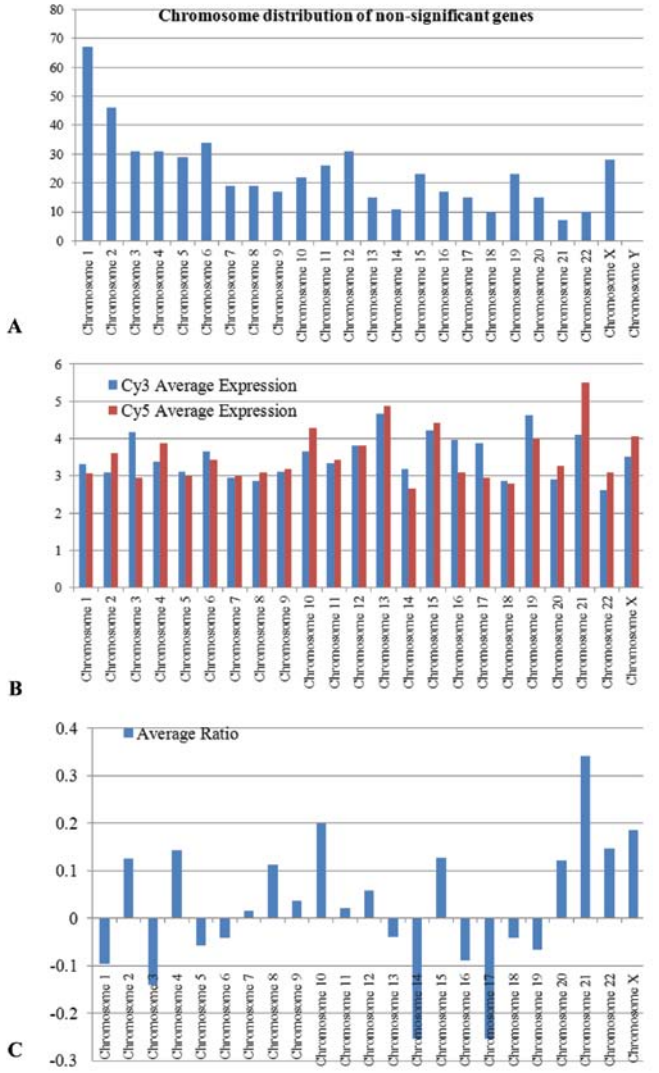

Figure 9. Chromosome distribution of (A) non-significant genes, (B) with average expression for each channel separately and (C) gene ratios.

ratios, as well as the non-significant genes between all comparisons. Analysis of the DEGs revealed 31 TFs with a FDR of 4% for $p<0.01$ (Fig. 11A). In particular, an interesting case was the prediction of STAT6, which regulates DLC1 and WNT5A genes. Of these TFs, several displayed intriguing behavioral patterns, since they manifested an increased tendency in gene expression. Such examples were the RORA1, NFY and ERR1 TFs (Fig. 12). On the other hand, analysis of all common non-significant genes predicted 329 TFs with $p<0.01$ and a FDR of <1% (Fig. 11B). Attention was drawn to three TFs: STAT, GR and NFκB (Fig. 11C). These TFs regulate genes in the two cell types in the same manner, assuming that they play an equal role in gene regulation (Fig. 12). In particular, STAT is part of the JAK-STAT-MAPK pathway, which is considered to be of outermost importance in the regulation of carcinogenesis and tumor progression.

GO. GO analysis was used in order to approach the functionality of the DEGs. As previously described two gene groups were used: i) The DEGs for each channel separately as well as DEGs for samples ratio and ii) GO analysis for the commonly

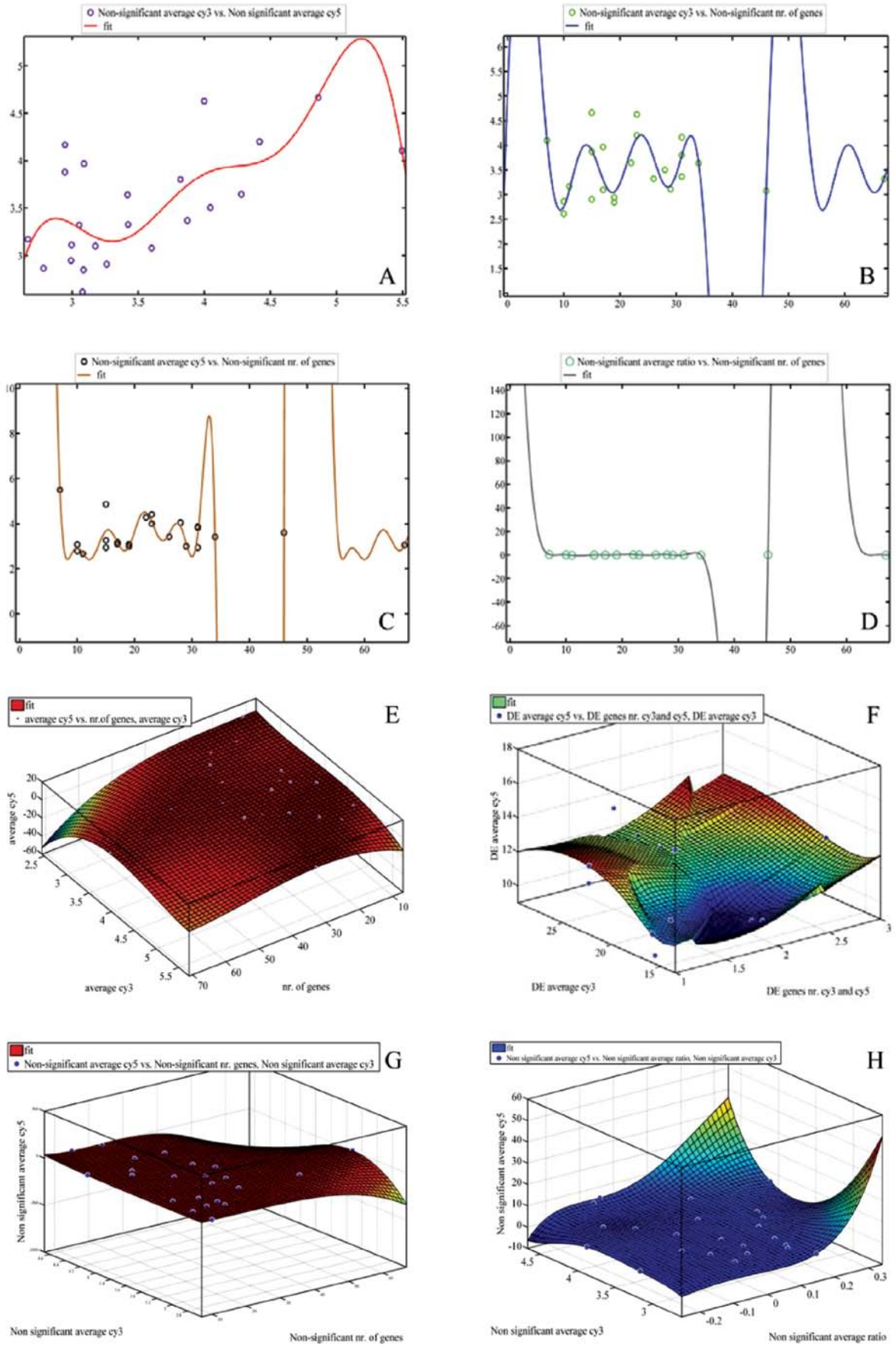

Figure 10. Fittings of chromosome distributions. (A) Curve fitting of the non-significant genes under Cy3 and non-significant genes under Cy5. (B) Curve fittings of non-significant genes under Cy3 and number of genes per chromosome. (C) Curve fittings of non-significant genes under Cy5 and number of genes per chromosome. (D) Curve fittings of non-significant genes ratios and number of genes per chromosome. (E) 3D fittings of average Cy5, number of genes and average Cy3. (F) 3D fittings of number of DEGs, average Cy5 and average Cy3 intensities. (G) 3D fittings of non-significant number of genes, non-significant average Cy5 and non-significant average Cy3 intensities. (H) 3D fittings of non-significant genes ratios, non-significant average Cy5 and non-significant average Cy3 intensities.

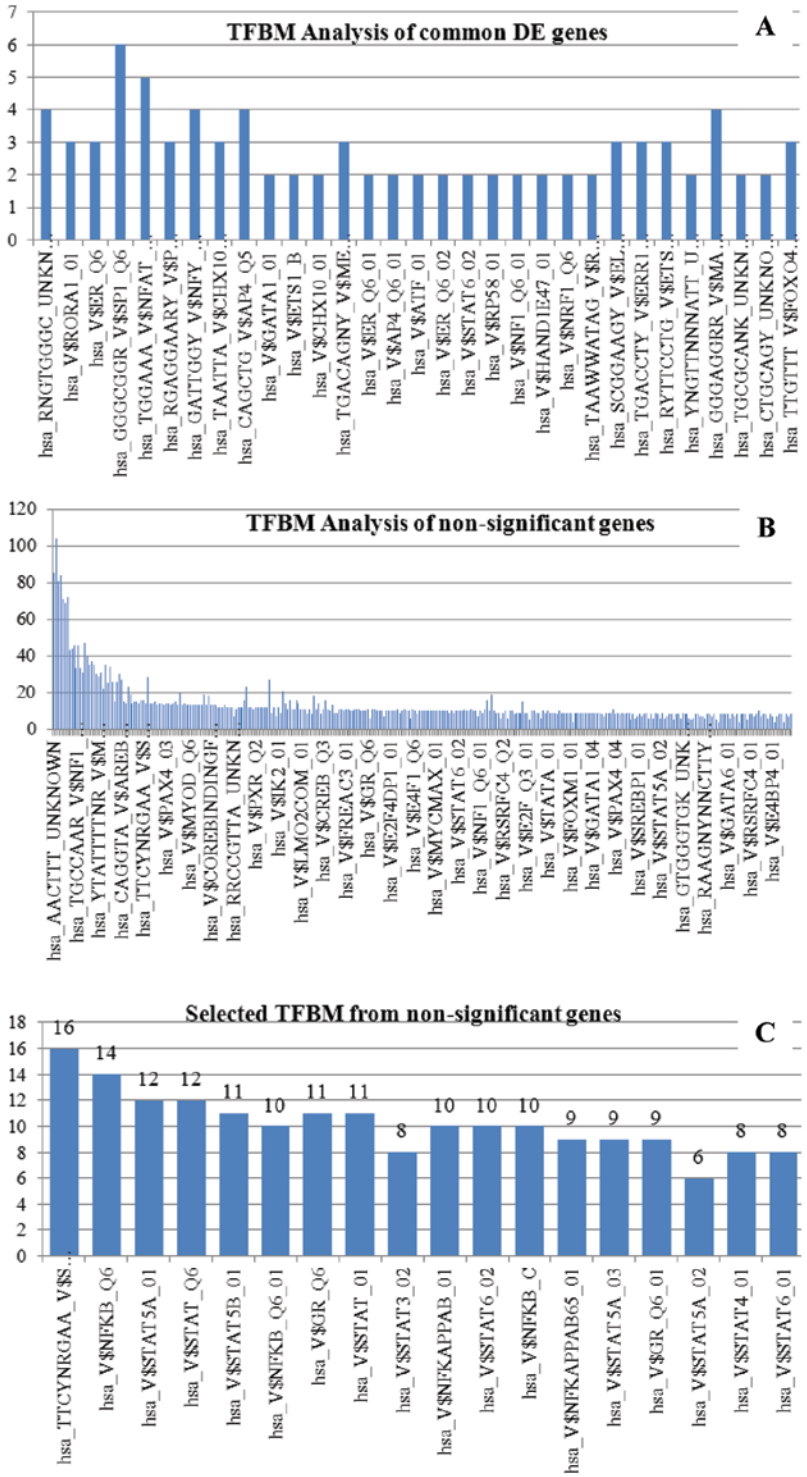

Figure 11. TFBM analysis of (A) common DEGs as well as (B and C) non-significant genes. DE, differentially expessed.

non-significant genes. GO relations for the general categories of biological process, cellular compartment and molecular function are presented in Fig. 13A and B. DEGs were predicted to participate in two main functions ($p<0.01$), receptor binding and cytokine receptor binding (Fig. 13A). The detailed list of DEGs and GO entities prediction is presented in Table II. On the other hand, the non-significant genes consisted a larger dataset and we expected to find more predicted functions. The genes of interest were those that participate in biological process, particularly in proliferation, cell cycle, differentiation, communication (extracellular cell-cell signaling) and embryonal development.

Genes were divided into nine major categories based on their function and unchanged expression profiles: i) Secretion molecule genes: CGRRF1, IGFBP7, PDGFB, PRC1, TGFB3 and VEGFC, ii) receptor/receptor binding/cytokine activity

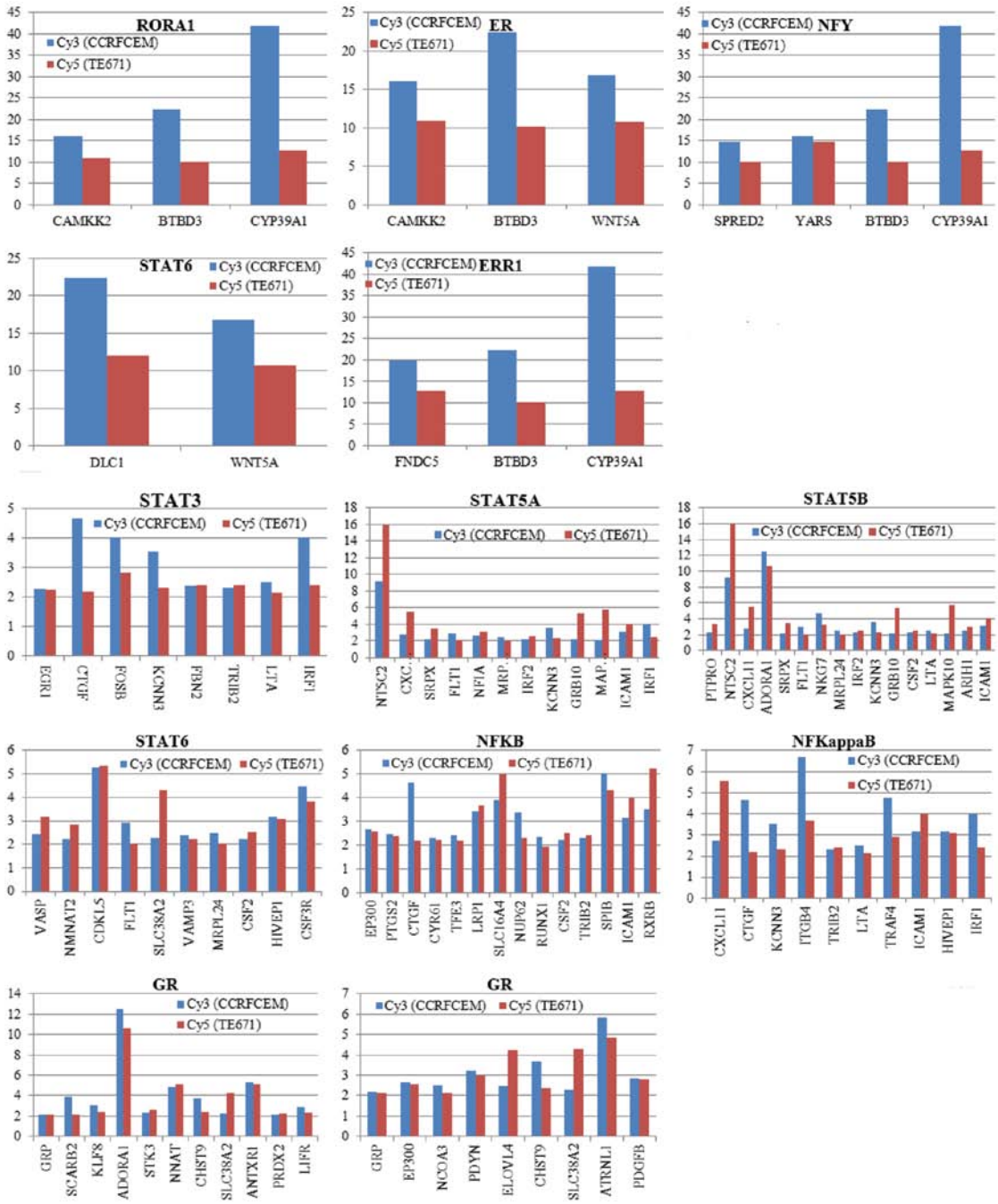

Figure 12. TFs of common non-significant genes. Emphasis was given to STAT, GR and NF-κB.

Table II. GO functions of differentially expressed genes.

Molecular function - cytokine receptor binding - GO:0005126 C=178; O=3; E=0.22; R=13.63; rawP=0.0013; adjP=0.0377				
FEM1B	10116	ENSG00000169018	FEM1B	Fem-1 homolog b (*C. elegans*)
SPRED2	200734	ENSG00000198369	SPRED2	Sprouty-related, EVH1 domain containing 2
YARS	8565	ENSG00000134684	YARS	Tyrosyl-tRNA synthetase
Molecular function - receptor binding - GO:0005102 C=856; O=5; E=1.06; R=4.72; rawP=0.0032; adjP=0.0464				
FEM1B	10116	ENSG00000169018	FEM1B	Fem-1 homolog b (*C. elegans*)
SPRED2	200734	ENSG00000198369	SPRED2	Sprouty-related, EVH1 domain containing 2
YARS	8565	ENSG00000134684	YARS	Tyrosyl-tRNA synthetase
NPFF	8620	ENSG00000139574	NPFF	Neuropeptide FF-amide peptide precursor
WNT5A	7474	ENSG00000114251	WNT5A	Wingless-type MMTV integration site family, member 5A

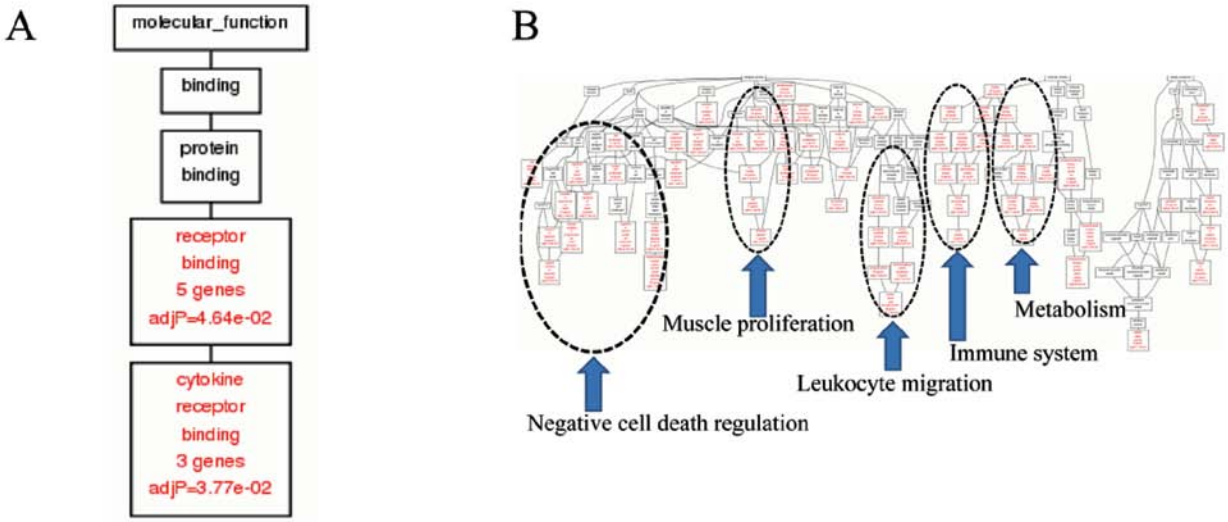

Figure 13. GO terms prediction for (A) DEGs and (B) non-significant genes.

genes: PDGFB, TGFB3, VEGFC, ADORA1, ALCAM, AVPR1A, CCRL1, CD40LG, CNR1, CSF3R, GABRA2, GLRA3, GPR44, HTR2B, IL2RA, IL9, LIFR, LRP1, MET, NPFF, PDYN, PTPN13, PTPN9, PTPRCAP, RXRB, SPRED2, TFRC, TLR3 and TRIP13, iii) cell communication/cell-cell signaling genes: TGFB3, GABRA2, HTR2B, LIFR, NPFF, PDYN, SPRED2, ARHGAP6, CDC2, DDEF1, DDEF2, EFA6R, GNG12, KIAA0974, PLEKHG1, PSMA4, RAPGEF2, RUNDC3A, TIAM1 and TMEPAI, iv) cell cycle genes, including genes for mitosis regulation and cell cycle process, such as: CDC2, PRC1, AK021716, DLGAP5, H2AFV, PPAPDC1B and ZZEF1, v) cell proliferation genes: CDC2, GNL3 and PDGFB, vi) cell differentiation/developmental/embryonic process genes: CDC2, VEGFC, CD40LG, IL2RA, ANXA4, BNIP3L, CD36, CFDP1, CUL7, FEM1B, FOXO1, MAB21L1, MBNL3, MMP2, NNAT, NP25, PDCD5, PDLIM7, PLAC1, RPS6KA3, RTTN, TCL1A, THBS4 and ZNF313, vii) stem cell/stem cell differentiation-related genes: CDC2, VEGFC, CD40LG, IL2RA, ANXA4, CFDP1, CUL7, FOXO1, MMP2, NNAT, NP25, PDCD5, PDLIM7, TCL1A, PDGFB, PRC1, DLGAP5, TGFB3, GABRA2, HTR2B, LIFR, NPFF, ARHGAP6, DDEF2, ADORA1, CCRL1, CNR1, CSF3R, GPR44, IL9, LRP1, MET, PTPN13, PTPN9, PTPRCAP, RXRB, TFRC, TLR3, CGRRF1, IGFBP7, FOSB, SIRT5 and TCF4. Also, in order to investigate the presence of negative or positive regulatory mechanisms, two more gene groups which are negative and positive regulators of cellular processes, were studied: ANXA4, CD36, FOSB, SIRT5 and TCF4 (negative regulatory genes) and FEM1B (positive regulator), viii) negative cell death regulatory genes: IL7, ADAM17, ACVR1, TNFAIP3, ANXA4, DHCR24, LRP1, BNIP3L, SELS, CSF2, NAIP, GSTP1, HMOX1, BARD1, PRDX2, CDC2, XRCC5, FNTA, ADORA1, PTEN, CFDP1, TGFB3, IGF1, DAPK1, MSH2, NUP62, CDKN2D, KIT and LIFR, ix) muscle proliferation genes, which is noteworthy as these genes are common to both cell types: IFNG, PTGS2, TGFBR3, ANG, FLT1, STAT1, IGF1, TGFB2, PDGFB and IL12B, x) genes involved in leukocyte migration, again an interesting observation as this function is common to both cell types: IFNG, ADAM17, ADORA1, SELP, ITGA6, IL8, TGFB2, CD34, HMOX1, PDGFB and ICAM1 and xi) genes involved in metabolism: PTPRO, MTM1, ACVR1, PTPRA, NTRK3, NDUFAB1, PDGFB, MAPK14, FLT3, BARD1, CDKN2C, RPS6KA2, TGFBR3, CDKL5, IGF1, EPHB6, MET, FGF23, MAP3K10, CDKN2D, GPD1L, KIT, IFNG, TNK2, PTPN9, TLK1, LRP1, KALRN, CDC2, ATP5F1, DCLK1, FLT1, MADD, STAT1, PPP1CB, MAPK13, MAPK10, PARD3, DYRK3, NDUFS1, TRIB2, TGFB2, INPP1, PIP4K2A, ADORA1, ANG, STK3, FLT4, PTEN, MSH2, DAPK1, TGFB3, SYNJ2, CSNK2A2, MORC3, VEGFC, PDGFC, ADAM17, PIK3C3, MAPKAPK3, PTPN13, CSF2, PRDX2, DOCK7, FGR, PGK1, TIE1, NUP62, STK25, CCL11, RPS6KA3 and CSF1R. The detailed results of the GO analysis for non-significant genes are presented in Table III. The tables is presented in such a way that the overlapping functions of genes is shown. We focused on genes specific for leukemia and RMS, and their relations to secretion, receptors, cell cycle, cell proliferation, cell differentiation and cell death regulation. Genes shown in bold are those considered to be unchanged or equally regulated in both cell types.

Pathway analysis. In order to understand the common mechanics of the two different types of cancer and find potential oncogenic drivers, a pathway analysis was applied. The purpose was to identify genes that participate in various pathways and the way they interact among them. Due to the complexity of the pathways and the transcripts revealed by the microarrays, we used the following approach for this analysis: First, genes were separated in two categories (DEGs and non-significant genes). Second, using the Pathway Explorer and WebGestalt tools, we explored the occurrence of the genes revealed in the microarrays, in known pathways from all available databases. DEGs revealed one significant pathway, the JAK-STAT-MAPK pathway ($p<0.01$), with the participation of SPRED2 and IL2RA. On the other hand, the non-significant genes were predicted to participate in a plethora of pathways (Fig. 14). An overview of the pathway predictions based on the KEGG pathway

Table III. Detailed results of the GO analysis for non-significant genes.

Unique ID	Gene name	Secretion molecule	Receptor/ receptor binding/ cytokine activity	Cell communication/ cell-cell signaling	Cell cycle	Cell proliferation	Cell differentiation/ developmental process/ embryonic development	Negative regulation of cellular process	Positive regulation of cellular process	Stem cell/ stem cell differentiation	Negative cell death reguation	Muscle proliferation	Leukocyte migration	Metabolism	Fold expression
NM_000674	**ADORA1**		**X**							**X**					**0.35570**
AK021716	AK021716				X										0.10320
Y10183	**ALCAM**		**X**												**0.80360**
NM_001153	ANXA4						X	X		X					-0.41550
NM_001174	**ARHGAP6**			**X**						**X**					**-0.00700**
NM_000706	AVPR1A		X												0.08890
AL132665	**BNIP3L**						**X**								**-0.38220**
NM_016557	CCRL1		X							X					-0.24970
BX091860.1	**CD36**						**X**	**X**							**-0.11330**
NM_000074	CD40LG		X				X			X					0.92110
NM_001786	**CDC2**			**X**	**X**	**X**	**X**			**X**					**-0.28130**
NM_006324	CFDP1						X			X					-0.10830
NM_006568	**CGRRF1**	**X**								**X**					**0.38330**
NM_016083	CNR1		X							X					0.96720
NM_000760	**CSF3R**		**X**							**X**					**0.18160**
NM_014780	CUL7						X			X					-0.65120
AB033075	**DDEF1**			**X**											**0.15180**
NM_003887	DDEF2			X						X					0.46100
NM_014750	**DLGAP5**				**X**					**X**					**-0.16760**
NM_015310	EFA6R			X											-0.85590
AB007856	**FEM1B**		**X**	**X**			**X**		**X**						**0.09350**
NM_006732	FOSB							X		X					0.59260
NM_002015	**FOXO1**						**X**			**X**					**-0.52260**
NM_000807	GABRA2		X	X						X					-0.11640
NM_006529	**GLRA3**		**X**												**-0.17370**
AK055914	GNG12			X											0.88830
NM_014366	**GNL3**					**X**									**0.19610**
NM_004778	GPR44		X							X					-0.81440
AK025785	**H2AFV**				**X**										**-0.13740**
NM_000867	HTR2B		X	X						X					-0.69180
NM_001553	**IGFBP7**	**X**								**X**					**0.65840**
NM_000417	IL2RA		X				X			X					-0.05850
NM_000590	**IL9**		**X**							**X**					**-0.08720**
BC015394	KIAA0974			X											0.25090
NM_002310	**LIFR**		**X**	**X**						**X**					**0.05560**
NM_002332	LRP1		X							X					0.96870
NM_005584	**MAB21L1**						**X**								**-0.21650**
AL133625	MBNL3						X								0.59340
NM_000245	**MET**		**X**							**X**					**-0.88820**

Table III. Continued.

Unique ID	Gene name	Secretion molecule	Receptor/ receptor binding/ cytokine activity	Cell communication/ cell-cell signaling	Cell cycle	Cell proliferation	Cell differentiation/ developmental process/ embryonic development	Negative regulation of cellular process	Positive regulation of cellular process	Stem cell/ stem cell differentiation	Negative cell death reguation	Muscle proliferation	Leukocyte migration	Metabolism	Fold expression
NM_004530	MMP2						X			X					-0.28880
NM_005386	**NNAT**						**X**			**X**					**-0.69920**
NM_013259	NP25						X			X					0.23170
NM_003717	**NPFF**		**X**	**X**						**X**					**0.18860**
NM_004708	PDCD5						X			X					0.09580
NM_002608	**PDGFB**	**X**	**X**			**X**				**X**					**-0.78240**
NM_005451	PDLIM7						X			X					-0.27470
NM_024411	**PDYN**		**X**	**X**											**0.49460**
NM_021796	PLAC1						X								-0.14430
AB033035	**PLEKHG1**			**X**											**0.30110**
NM_032483	PPAPDC1B				X										0.30310
NM_003981	**PRC1**	**X**			**X**					**X**					**0.39000**
AK055714	PSMA4			X											-0.89000
NM_006264	**PTPN13**		**X**							**X**					**-0.17040**
NM_002833	PTPN9		X							X					-0.51980
NM_005608	**PTPRCAP**		**X**							**X**					**-0.29690**
NM_014247	RAPGEF2			X											-0.37350
AK022869	**RPS6KA3**						**X**								**0.48650**
BC007359	RTTN						X								0.23600
NM_006695	**RUNDC3A**			**X**											**0.97270**
NM_021976	RXRB		X							X					-0.91460
NM_031244	**SIRT5**							**X**		**X**					**-0.21510**
AK056479	SPRED2		X	X											-0.24150
NM_003199	**TCF4**							**X**		**X**					**0.78030**
NM_021966	TCL1A						X			X					0.21240
NM_003234	**TFRC**		**X**							**X**					**-0.18980**
NM_003239	TGFB3	X	X	X						X					0.87070
NM_003248	**THBS4**						**X**								**-0.49600**
U90902	TIAM1			X											-0.72830
NM_003265	**TLR3**		**X**							**X**					**0.49000**
AF305616	TMEPAI			X											0.01560
NM_004237	**TRIP13**		**X**												**0.18310**
NM_005429	VEGFC	X	X				X			X					0.20610
BC013695	**ZNF313**						**X**								**-0.44100**
AB007859	ZZEF1				X										0.01690
NM_003680	**YARS**		**X**	**X**											**-0.11518**
NM_03392	WNT5A		X	X											-0.64908

The overlapping functions of genes are presented. Genes shown in bold are those considered to be unchanged or equally regulated in both cell types.

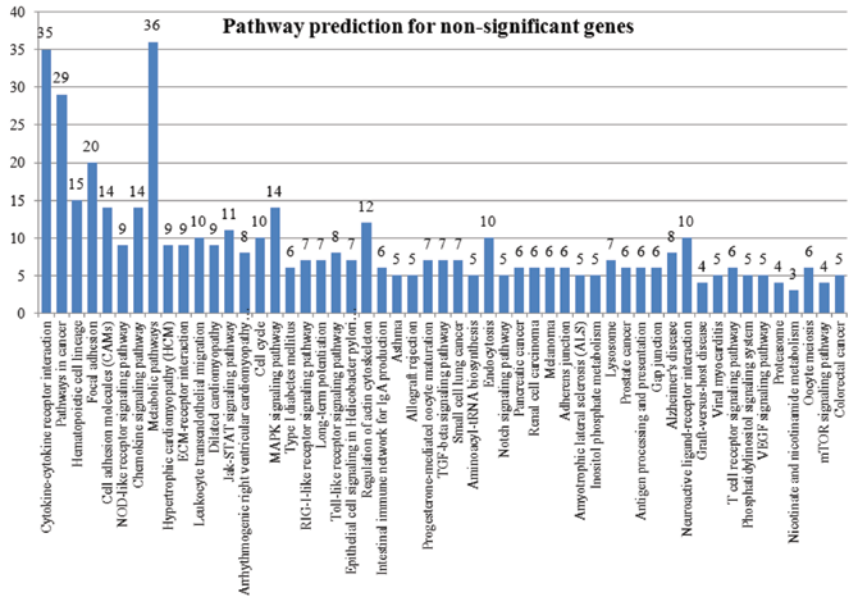

Figure 14. Prediction of pathway participation of non-significant genes. Numbers over the bars indicate the numbers of genes found on each pathway with a 99% confidence interval.

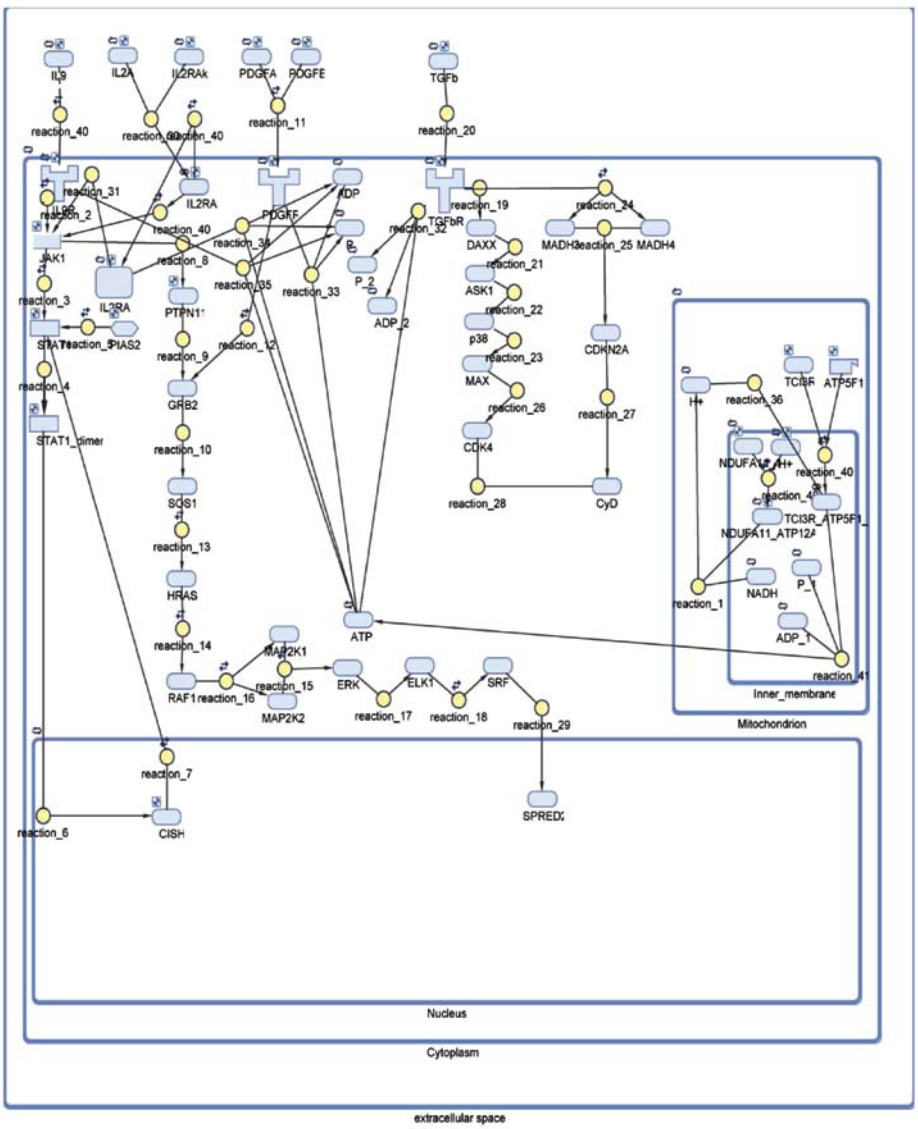

Figure 15. Diagrammatic view of the coupled pathways used for simulation.

database and the pathways of interest are depicted in Table IV. Thereafter, we analyzed the common presence of extracellular signal molecules. The two cell types share three main axons of signaling, for cell cycle regulation and cell proliferation, among others: i) an ECM-receptor/focal adhesion/MAPK signal transduction pathway, ii) a cytokine-cytokine-receptor/MAPK/cell cycle signal transduction pathway, iii) cell death regulatory mechanisms and iv) a JAK-STAT/MAPK signal transduction pathway. All these combinations participate in cell proliferation, differentiation, cell fate determination and anti-apoptosis. In order to gain further insight into gene regulatory mechanisms common to both cell types, we performed a pathway simulation including genes of interest from all pathways. Furthermore, we attempted to model the investigated pathways using simulations. We created a coupled pathway, which included the JAK-STAT, MAPK, TGF-β signaling pathways and basic metabolism pathways (Fig. 15). Further simulations of the pathway manifested very interesting results. Four molecules appeared to manifest oscillations in their behavior: JAK, STAT1 and PIAS2 (part of the JAK-STAT pathway) and CDK4 (part of the TGF-β pathway) (Fig. 16A). It appeared that these molecules followed rapid oscillatory dynamics and without an inhibitory mechanism, they constitute potential drivers of cellular proliferation. It is suggested that these four molecules are possible oncogenic drivers in the cell systems under study. Of note, our microarray analysis revealed that these four genes participate similarly in the two cell types. Since we defined the initial dynamics of these molecules, we investigated whether they follow linear or non-linear dynamics, and whether further correlations exist among them. In order to do so, we used state-space plots of combinations of the 4 genes. Of note, plotting JAK1 vs. STAT1 showed that they follow very complicated dynamics, which actually resemble a repeller or a 'source' (Fig. 16B). Similar behavior was manifested by the comparison of PIAS2 with STAT1 (Fig. 16C) and PIAS2 with JAK1 (Fig. 16D). Also, we observed that JAK1 vs. STAT1 and PIAS2 vs. JAK1 are almost mirror images of each other. On the contrary, plotting CDK4 vs. JAK1 did not reveal similar behavior, revealing a 'sink' effect that common drivers tend to collide (Fig. 16E). These results point towards chaotic phenomena (in terms of chaos dynamics). Further investigation is required in order to futher analyze the dynamics revealed in this study and clarify this phenomenon.

In order to examine the synergistic effects of the molecules, we simulated the sum these molecules with respect to time. Of note, the sum of STAT1 and JAK1 (Fig. 16F) manifested very similar behavior with the sum of PIAS2 and STAT1 (Fig. 16G), indicating that these molecules are possibly key molecules to the pathway function. Once again, the sum of JAK1 and STAT1 (Fig. 16F) was a mirror image to the sum of JAK1 and PIAS2 (Fig. 16H). Finally, the simulation of the sum of JAK1 and CDK4 indicated that it leads the system to an oscillatory behavior tending to infinity (Fig. 16I). This reinforces the role of the JAK1 and CDK4 molecules as potential oncogenic drivers of the cell types presented in our study.

Discussion

In the present study, we used computational and system biology approaches in order to investigate the following: i) In a certain gene set, genes that are specific to each cell type and at the same time common to both cell types, ii) similarities in tumor progression, cell cycle and secretory extracellular signaling, iii) common regulatory mechanisms for the two cell types, based on their expression profiles, iv) pathways common to both cell types, and v) evidence of the role of stem cells in tumorigenesis. For this purpose, we analyzed different signaling pathways and searched for the most prevalent pathway in the progression of the two cell types.

ALL and RMS are two malignancies originating from different cell types (a lymphoblast and a myoblast, respectively), although they both are of mesodermal origin. Understanding the origin of tumors on the 'poiesis' level, such as hemopoiesis/lymphopoiesis (76) or myogenesis, may lead to the discovery of new therapeutic targets. Therefore, we hypothesized that the two cell types possess common characteristics, first due to their common developmental origin and second, due to their malignant character. Therefore, we used microarrays and a bioinformatics approach in order to examine whether common genes that participate in critical cellular pathways exist between the two cell types.

Cytokine/cytokine interactions

Interleukins. Our analysis predicted 35 unique targets mapped on the cytokine/cytokine-receptor pathway. Cytokines are significant molecules participating in hemopoietic stem cell differentiation. In particular, γ interleukins were reported to have proliferative and differentiating effects on T-ALL primary cells (77). Despite the differences between normal blood stem cells and malignant ones, they both use cytokine signaling for progression and differentiation (78). Our analysis predicted IL8, IL9 and the IL2 receptor.

Chemokines. None of the CXCL or CXCR family of molecules appeared to have similar expression. It has been previously reported that in order for certain cell lines to produce these chemokines, the constitutive presence of NF-κB in the nucleus is required (79). The CCRF-CEM cells have shown that NF-κB is constitutively present in the nucleus (data not shown) supporting the evidence of chemokine expression. The fact that the NF-κB factor was predicted from TFBM analysis supports this hypothesis.

Hematopoietins. The two cell types seem to share a common expression profile for the LIFR gene. The LIFR protein participates in embryo implantation, in the differentiation of neural stem cells to astrocytes (80), as well as in the mesenchyme to epithelial conversion (81). Its role has been reported to be connected to the PTEN-Akt-FOXO axis and STAT3 (80). So far, there are no reports of the role of LIFR in ALL or RMS; its role is yet unclear in the present system. Another interesting gene our analysis predicted is CSF3R. It has been reported for its role in hematopoiesis, since it is expressed only in the myeloid lineages of hematopoietic cells (82). There are no reports linking CSF3R to RMS. However, a common developmental mechanism utilized by both cell types for their progression and growth, could exist.

PDGF family. Our study predicted that within the PDGF family, the two cell types share a common expression profile for the secretory molecules, PDGFB and VEGFC; as well as for the receptors, MET and FLT3. PDGF regulates clonal proliferation in pre-B cell lines and it has been found to be overexpressed in B-chronic leukemia (83). It has also been

Table IV. Prediction of pathway participation of non-significant genes at a 99% confidence interval.

KEGG pathway - cytokine-cytokine receptor interaction - 04060			
C=267; O=35; E=3.44; R=10.18; rawP=1.28e-24; adjP=1.42e-22			
ACVR1	90	ACVR1	Activin A receptor, type I
XCL1	6375	XCL1	Chemokine (C motif) ligand 1
TGFB2	7042	TGFB2	Transforming growth factor β2
TNFSF8	944	TNFSF8	Tumor necrosis factor (ligand) superfamily, member 8
CXCR3	2833	CXCR3	Chemokine (C-X-C motif) receptor 3
FLT3	2322	FLT3	Fms-related tyrosine kinase 3
PDGFB	5155	PDGFB	Platelet-derived growth factor β polypeptide [simian sarcoma viral (v-sis) oncogene homolog]
CSF3R	1441	CSF3R	Colony stimulating factor 3 receptor (granulocyte)
CCL26	10344	CCL26	Chemokine (C-C motif) ligand 26
FLT4	2324	FLT4	Fms-related tyrosine kinase 4
CCL8	6355	CCL8	Chemokine (C-C motif) ligand 8
TGFB3	7043	TGFB3	Transforming growth factor β3
CD70	970	CD70	CD70 molecule
MET	4233	MET	Met proto-oncogene (hepatocyte growth factor receptor)
KIT	3815	KIT	V-kit Hardy-Zuckerman 4 feline sarcoma viral oncogene homolog
IL7	3574	IL7	Interleukin 7
IFNG	3458	IFNG	Interferon γ
VEGFC	7424	VEGFC	Vascular endothelial growth factor C
PDGFC	56034	PDGFC	Platelet derived growth factor C
CXCL13	10563	CXCL13	Chemokine (C-X-C motif) ligand 13
IFNGR2	3460	IFNGR2	Interferon γ receptor 2 (interferon γ transducer 1)
CCL20	6364	CCL20	Chemokine (C-C motif) ligand 20
CNTFR	1271	CNTFR	Ciliary neurotrophic factor receptor
IL9	3578	IL9	Interleukin 9
CSF2	1437	CSF2	Colony stimulating factor 2 (granulocyte-macrophage)
IL12B	3593	IL12B	Interleukin 12B (natural killer cell stimulatory factor 2, cytotoxic lymphocyte maturation factor 2, p40)
CXCL11	6373	CXCL11	Chemokine (C-X-C motif) ligand 11
IL8	3576	IL8	Interleukin 8
FLT1	2321	FLT1	Fms-related tyrosine kinase 1 (vascular endothelial growth factor/vascular permeability factor receptor)
CXCL1	2919	CXCL1	Chemokine (C-X-C motif) ligand 1 (melanoma growth stimulating activity α)
IL17A	3605	IL17A	Interleukin 17A
LTA	4049	LTA	Lymphotoxin α (TNF superfamily, member 1)
CCL11	6356	CCL11	Chemokine (C-C motif) ligand 11
LIFR	3977	LIFR	Leukemia inhibitory factor receptor α
CSF1R	1436	CSF1R	Colony stimulating factor 1 receptor
KEGG pathway - pathways in cancer - 05200			
C=330; O=29; E=4.25; R=6.82; rawP=7.35e-16; adjP=4.08e-14			
VEGFC	7424	VEGFC	Vascular endothelial growth factor C
EP300	2033	EP300	E1A binding protein p300
LAMA4	3910	LAMA4	Laminin, α4
COL4A2	1284	COL4A2	Collagen, type IV α2
ITGA6	3655	ITGA6	Integrin α6
CTNNA1	1495	CTNNA1	Catenin (cadherin-associated protein) α1, 102 kDa
TGFB2	7042	TGFB2	Transforming growth factor β2
GSTP1	2950	GSTP1	Glutathione S-transferase pi 1
FLT3	2322	FLT3	Fms-related tyrosine kinase 3
PDGFB	5155	PDGFB	Platelet-derived growth factor β polypeptide [simian sarcoma viral (v-sis) oncogene homolog]
CTNNA2	1496	CTNNA2	Catenin (cadherin-associated protein) α2
CSF3R	1441	CSF3R	Colony stimulating factor 3 receptor (granulocyte)
RXRB	6257	RXRB	Retinoid X receptor β
PTGS2	5743	PTGS2	Prostaglandin-endoperoxide synthase 2 (prostaglandin G/H synthase and cyclooxygenase)
PTEN	5728	PTEN	Phosphatase and tensin homolog
WNT5B	81029	WNT5B	Wingless-type MMTV integration site family, member 5B
IL8	3576	IL8	Interleukin 8
STAT1	6772	STAT1	Signal transducer and activator of transcription 1, 91kDa
IGF1	3479	IGF1	Insulin-like growth factor 1 (somatomedin C)
DAPK1	1612	DAPK1	Death-associated protein kinase 1
MSH2	4436	MSH2	MutS homolog 2, colon cancer, nonpolyposis type 1 (*E. coli*)
TGFB3	7043	TGFB3	Transforming growth factor β 3
RUNX1	861	RUNX1	Runt-related transcription factor 1

Table IV. Continued.

MET	4233	MET	Met proto-oncogene (hepatocyte growth factor receptor)
MAPK10	5602	MAPK10	Mitogen-activated protein kinase 10
FGF23	8074	FGF23	Fibroblast growth factor 23
KIT	3815	KIT	V-kit Hardy-Zuckerman 4 feline sarcoma viral oncogene homolog
TRAF4	9618	TRAF4	TNF receptor-associated factor 4
CSF1R	1436	CSF1R	Colony stimulating factor 1 receptor
KEGG pathway - hematopoietic cell lineage - 04640 C=88; O=15; E=1.13; R=13.23; rawP=4.99e-13; adjP=1.85e-11			
HLA-DRB1	3123	HLA-DRB1	Major histocompatibility complex, class II, DR β1
IL7	3574	IL7	Interleukin 7
CD8A	925	CD8A	CD8a molecule
ITGA4	3676	ITGA4	Integrin α4 (antigen CD49D, α4 subunit of VLA-4 receptor)
ITGA6	3655	ITGA6	Integrin α6
CD1C	911	CD1C	CD1c molecule
ITGB3	3690	ITGB3	Integrin β3 (platelet glycoprotein IIIa, antigen CD61)
CSF2	1437	CSF2	Colony stimulating factor 2 (granulocyte-macrophage)
CD1D	912	CD1D	CD1d molecule
CD34	947	CD34	CD34 molecule
FLT3	2322	FLT3	Fms-related tyrosine kinase 3
KIT	3815	KIT	V-kit Hardy-Zuckerman 4 feline sarcoma viral oncogene homolog
TFRC	7037	TFRC	Transferrin receptor (p90, CD71)
CSF1R	1436	CSF1R	Colony stimulating factor 1 receptor
CSF3R	1441	CSF3R	Colony stimulating factor 3 receptor (granulocyte)
KEGG pathway - metabolic pathways - 01100 C=1104; O=36; E=14.22; R=2.53; rawP=4.90e-07; adjP=6.80e-06			
NDUFS1	4719	NDUFS1	NADH dehydrogenase (ubiquinone) Fe-S protein 1, 75 kDa (NADH-coenzyme Q reductase)
PRDX6	9588	PRDX6	Peroxiredoxin 6
DHCR24	1718	DHCR24	24-Dehydrocholesterol reductase
ETNK1	55500	ETNK1	Ethanolamine kinase 1
ASL	435	ASL	Argininosuccinate lyase
APRT	353	APRT	Adenine phosphoribosyltransferase
NDUFAB1	4706	NDUFAB1	NADH dehydrogenase (ubiquinone) 1α/β subcomplex, 1, 8 kDa
INPP1	3628	INPP1	Inositol polyphosphate-1-phosphatase
PMM2	5373	PMM2	Phosphomannomutase 2
GSS	2937	GSS	Glutathione synthetase
ACSS2	55902	ACSS2	Acyl-CoA synthetase short-chain family member 2
SC4MOL	6307	SC4MOL	Sterol-C4-methyl oxidase-like
NMNAT2	23057	NMNAT2	Nicotinamide nucleotide adenylyltransferase 2
HMGCL	3155	HMGCL	3-Hydroxymethyl-3-methylglutaryl-Coenzyme A lyase
APIP	51074	APIP	APAF1 interacting protein
SYNJ2	8871	SYNJ2	Synaptojanin 2
ALDH18A1	5832	ALDH18A1	Aldehyde dehydrogenase 18 family, member A1
GATM	2628	GATM	Glycine amidinotransferase (L-arginine:glycine amidinotransferase)
PIK3C3	5289	PIK3C3	Phosphoinositide-3-kinase, class 3
FBP2	8789	FBP2	Fructose-1,6-bisphosphatase 2
ECHS1	1892	ECHS1	Enoyl Coenzyme A hydratase, short chain, 1, mitochondrial
AK3L1	205	AK3L1	Adenylate kinase 3-like 1
HYI	81888	HYI	Hydroxypyruvate isomerase homolog (*E. coli*)
BST1	683	BST1	Bone marrow stromal cell antigen 1
H6PD	9563	H6PD	Hexose-6-phosphate dehydrogenase (glucose 1-dehydrogenase)
ATP5F1	515	ATP5F1	ATP synthase, H^+ transporting, mitochondrial F0 complex, subunit B1
ADSS	159	ADSS	Adenylosuccinate synthase
MGAT2	4247	MGAT2	Mannosyl (α-1,6-)-glycoprotein β-1,2-N-acetylglucosaminyltransferase
NT5C2	22978	NT5C2	5'-nucleotidase, cytosolic II
EPRS	2058	EPRS	Glutamyl-prolyl-tRNA synthetase
PGK1	5230	PGK1	Phosphoglycerate kinase 1
G6PD	2539	G6PD	Glucose-6-phosphate dehydrogenase
MAOA	4128	MAOA	Monoamine oxidase A
HK1	3098	HK1	Hexokinase 1
AMPD1	270	AMPD1	Adenosine monophosphate deaminase 1 (isoform M)
HAO1	54363	HAO1	Hydroxyacid oxidase (glycolate oxidase) 1

Table IV. Continued.

KEGG pathway - JAK-STAT signaling pathway - 04630 C=155; O=11; E=2.00; R=5.51; rawP=6.00e-06; adjP=5.00e-05			
IFNG	3458	IFNG	Interferon γ
EP300	2033	EP300	E1A binding protein p300
IL7	3574	IL7	Interleukin 7
IFNGR2	3460	IFNGR2	Interferon γ receptor 2 (interferon γ transducer 1)
STAT1	6772	STAT1	Signal transducer and activator of transcription 1, 91 kDa
CNTFR	1271	CNTFR	Ciliary neurotrophic factor receptor
IL9	3578	IL9	Interleukin 9
CSF2	1437	CSF2	colony stimulating factor 2 (granulocyte-macrophage)
LIFR	3977	LIFR	Leukemia inhibitory factor receptor α
IL12B	3593	IL12B	Interleukin 12B (natural killer cell stimulatory factor 2, cytotoxic lymphocyte maturation factor 2, p40)
CSF3R	1441	CSF3R	Colony stimulating factor 3 receptor (granulocyte)
KEGG pathway - cell cycle - 04110 C=128; O=10; E=1.65; R=6.07; rawP=6.78e-06; adjP=5.02e-05			
EP300	2033	EP300	E1A binding protein p300
CDKN2C	1031	CDKN2C	Cyclin-dependent kinase inhibitor 2C (p18, inhibits CDK4)
BUB3	9184	BUB3	Budding uninhibited by benzimidazoles 3 homolog (yeast)
TGFB3	7043	TGFB3	Transforming growth factor β3
ORC1L	4998	ORC1L	Origin recognition complex, subunit 1-like (yeast)
TGFB2	7042	TGFB2	Transforming growth factor β2
CDKN2D	1032	CDKN2D	Cyclin-dependent kinase inhibitor 2D (p19, inhibits CDK4)
CDC2	983	CDC2	Cell division cycle 2, G1 to S and G2 to M
MCM3	4172	MCM3	Minichromosome maintenance complex component 3
RAD21	5885	RAD21	RAD21 homolog (S. pombe)
KEGG pathway - MAPK signaling pathway - 04010 C=269; O=14; E=3.46; R=4.04; rawP=1.25e-05; adjP=8.67e-05			
RPS6KA2	6196	RPS6KA2	Ribosomal protein S6 kinase, 90 kDa, polypeptide 2
STK3	6788	STK3	Serine/threonine kinase 3 (STE20 homolog, yeast)
MAPKAPK3	7867	MAPKAPK3	Mitogen-activated protein kinase-activated protein kinase 3
RAPGEF2	9693	RAPGEF2	Rap guanine nucleotide exchange factor (GEF) 2
CACNB2	783	CACNB2	Calcium channel, voltage-dependent β2 subunit
TGFB3	7043	TGFB3	Transforming growth factor β3
PPP3CC	5533	PPP3CC	Protein phosphatase 3 (formerly 2B), catalytic subunit, γ isoform
MAPK13	5603	MAPK13	Mitogen-activated protein kinase 13
TGFB2	7042	TGFB2	Transforming growth factor β2
MAPK10	5602	MAPK10	Mitogen-activated protein kinase 10
FGF23	8074	FGF23	Fibroblast growth factor 23
MAPK14	1432	MAPK14	Mitogen-activated protein kinase 14
PDGFB	5155	PDGFB	Platelet-derived growth factor β polypeptide [simian sarcoma viral (v-sis) oncogene homolog]
RPS6KA3	6197	RPS6KA3	Ribosomal protein S6 kinase, 90 kDa, polypeptide 3
KEGG pathway----Regulation of actin cytoskeleton----04810 C=216;O=12;E=2.78;R=4.31;rawP=2.73e-05;adjP=0.0002			
PDGFC	56034	PDGFC	platelet derived growth factor C
ARHGEF6	9459	ARHGEF6	Rac/Cdc42 guanine nucleotide exchange factor (GEF) 6
ITGA4	3676	ITGA4	Integrin α4 (antigen CD49D, α4 subunit of VLA-4 receptor)
ARHGEF7	8874	ARHGEF7	Rho guanine nucleotide exchange factor (GEF) 7
ITGA6	3655	ITGA6	Integrin α6
ITGB3	3690	ITGB3	Integrin β3 (platelet glycoprotein IIIa, antigen CD61)
PPP1CB	5500	PPP1CB	Protein phosphatase 1, catalytic subunit β isoform
ITGB4	3691	ITGB4	Integrin β4
PDGFB	5155	PDGFB	Platelet-derived growth factor β polypeptide [simian sarcoma viral (v-sis) oncogene homolog]
TIAM1	7074	TIAM1	T-cell lymphoma invasion and metastasis 1
FGF23	8074	FGF23	Fibroblast growth factor 23
PIP4K2A	5305	PIP4K2A	Phosphatidylinositol-5-phosphate 4-kinase, type IIα
KEGG pathway - proteasome - 03050 C=48; O=4; E=0.62; R=6.47; rawP=0.0034; adjP=0.0077			
IFNG	3458	IFNG	Interferon γ
POMP	51371	POMP	Proteasome maturation protein
PSMA2	5683	PSMA2	Proteasome (prosome, macropain) subunit α type, 2
PSME4	23198	PSME4	Proteasome (prosome, macropain) activator subunit 4

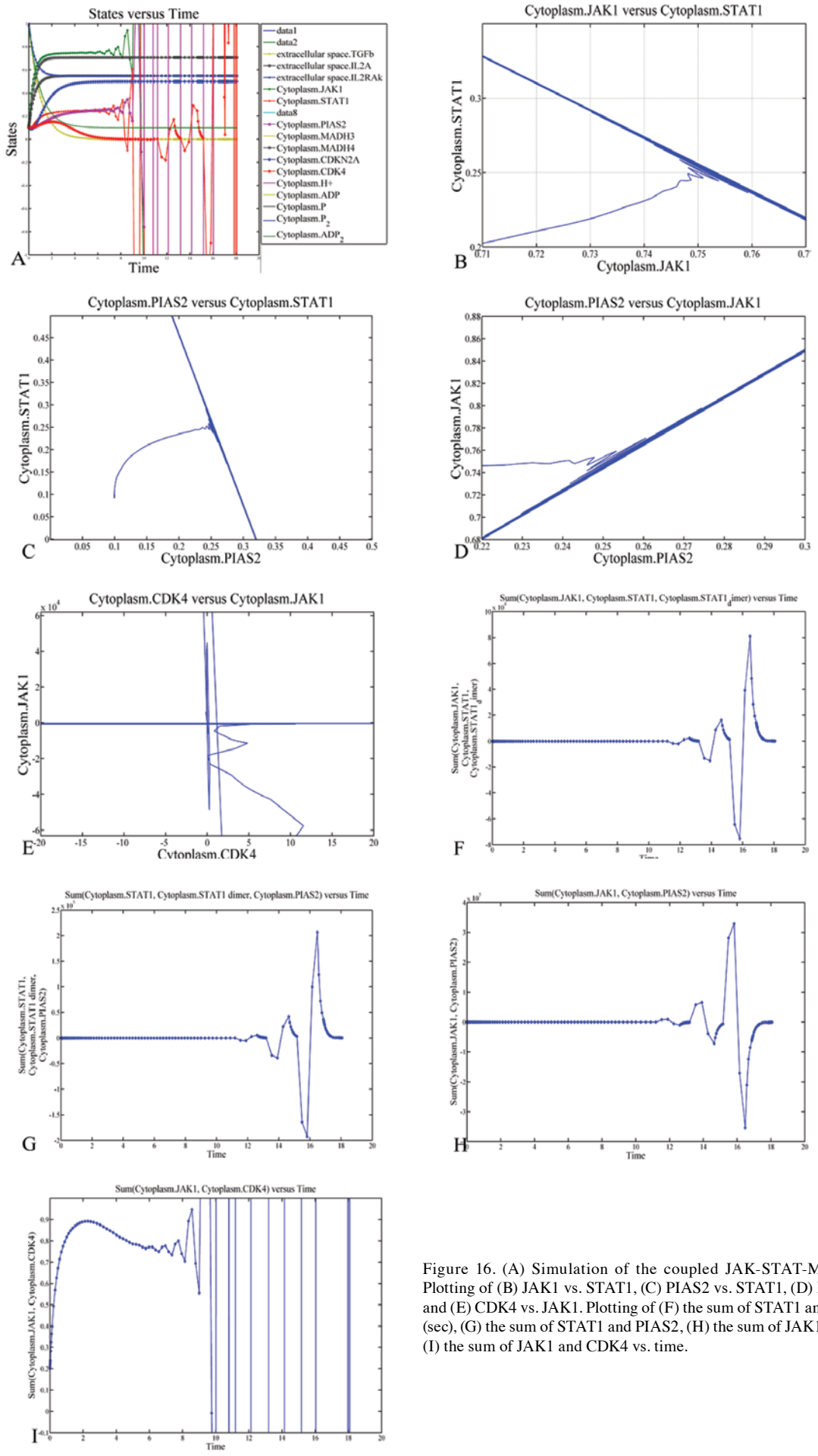

Figure 16. (A) Simulation of the coupled JAK-STAT-MAPK pathway. Plotting of (B) JAK1 vs. STAT1, (C) PIAS2 vs. STAT1, (D) PIAS2 vs. JAK1 and (E) CDK4 vs. JAK1. Plotting of (F) the sum of STAT1 and JAK1 vs. time (sec), (G) the sum of STAT1 and PIAS2, (H) the sum of JAK1 and PIAS2 and (I) the sum of JAK1 and CDK4 vs. time.

reported that both VEGF and PDGF families are involved in neo-angiogenesis in embryos and tumors (84). RMSs have been reported to express IGF and PDGF receptors (6). However, receptor expression is independent of signal molecule expression. The expression of PDGF has been associated with poor prognosis (6). MET is the receptor of the hepatocyte growth factor (produced by bone marrow stromal cells) (85) specific for the acute phase of T-ALL (86). It has also been reported to play a role in chronic myeloid leukemia (87) as well as to be expressed in B-ALL cells possessing the TEL-AML1 translocation, but not in B-ALL cells without this translocation (88). At the same time, FLT3 is known to cause AML when a mutation is present in this receptor (89). Members of the PDGF family of signaling molecules appear to be active in the two cell types studied. This suggests that both cell types utilize the same molecules for their signaling purposes. Since the PDGF family molecules are active in embryogenesis and hemopoietic cell differentiation, it can be assumed that in the present system, a developmental mechanism is still active after the occurrence of the malignancy.

ECM-receptor interactions. In this signaling pathway, the two cell types share two genes with equal expression: Thrombospondin-4 (THBS4) and integrin (ITGA6). ITGA6 is known to be expressed in childhood hematologic malignancies (90), whereas there are no reports linking THBS4 with leukemia or RMS. Both are signaling molecules, playing a role in ECM-receptor interaction.

Focal adhesion. Both the ECM-receptor and cytokine-receptor interaction signaling are interrelated to focal adhesion. Our system predicted two signal transduction pathways: The first includes the ECM-receptor signaling over LAMB2-ITGA6-CAPN2-VASP-cell motility and the second includes cytokine induction over VEGF-MET/ACK1/-ELK1-cell proliferation. Elk1 was not found to be expressed by the microarray screening but it was correctly predicted from the TFBM analysis.

CAPN2 is a known regulator of cell migration of various cell types (91) but its role in either leukemia or RMS is not reported. Similarly, for LAMB2 there are no known reports of its relation to leukemia or RMS. In our system, these two molecules were predicted to play a role in migration for the two cell types studied. ACK1 is a known cell cycle regulator whose overexpression is related with cancer and EGFR down-regulation (92,93). Of note, in the present system ACK1 was equivalently expressed, while EGFR was overexpressed in the TE-671 cells. Elk-1, the predicted TF, appears to be involved in direct association with the focal adhesion kinase and MAP kinase, inducing anti-apoptosis (94). There is a direct connection between the focal adhesion pathway and cell cycle regulation through the MAPK pathway. Our system correctly predicted that the mediator for this transition is the Elk-1 TF, for both cell types.

JAK-STAT/MAPK signaling pathways. Signaling in the JAK-STAT pathway was predicted to start with the interleukins IL2, IL8, IL9 and their receptors, common for both cell types. The interleukin receptor binds to the JAK kinase which activates by phosphorylation (95) the STAT1 TF (96,97). The STAT1 TF remains dormant in the cytoplasm until activated by JAK; then it translocates to the nucleus signaling the expression of genes responsible for proliferation, growth and differentiation. The STAT1 and STAT5B TFs appeared to be expressed in the present system, whereas STAT1 was also predicted by TFBM analysis. Both TFs were overexpressed in the TE-671 cells compared to CCRF-CEM. At the same time, both cell types express PIAS2 (PIASxα) a known STAT1 inhibitor acting as a E3 ligase (95). When STAT1 translocates to the nucleus it interacts with histone acetyltransferase (CREB-binding protein) co-factor (98) and NF-κB to initiate transcription (99). This part of the JAK-STAT pathway can initiate gene transcription leading to proliferation, differentiation and development. On the other hand, there is the alternative regulation of cell proliferation by cytokines through the activation of the MAPK pathway via protein tyrosine phosphatases and the Ras/MAPK pathway (100). The activation over the Ras/MAPK pathway involves signaling from cytokines such as PDGFA or PDGFB, both expressed in our system, the activation of HRAS and subsequent activation of RAF/MAPK/ERK also known to be involved in myeloid cell terminal differentiation (101). Following these events, a new protein of the serine/threonine kinases (RPS6KA3) is involved which participates in the Ras/Raf/MAPK pathway (102). RPS6KA3 interacts with CREB TF, predicted by TFBM analysis, leading to gene regulation concerning cell proliferation. Alternative to this is the activation of the Elk-1 TF from ERK kinase. The Elk-1 TF is phosphorylated by the MAP kinases (103) and recruited by the SRF TF (104,105). The SRF factor binds gene promoters that possess the serum response elements (SREs) in order to induce immediate early (IE) genes such as c-FOS and EGR-1 (106). Interestingly, the SRF TF was predicted by the TFBM analysis while the genes EGR-1, -2, -3, -4 and FOSB appeared to be expressed in our system. Alternatively, it has been reported that TGF-β activates the MAPK signaling pathway via the p38/MAPK pathway (107). Of note, TGF-β and p38 were expressed in the two cell types under study, and were equally regulated, suggesting thus, a common utilization of this pathway for cell proliferation. In particular, TGF-β activates members of the MAPK pathway such as c-JUN, which in turn activate the stress-activated kinase p38 (108-111). The p38 kinase is known to interact with Elk-1 and ATF-2 TFs (112-115). The ATF-2 TF was also predicted by the TFBM analysis.

The mechanisms described, appear to be common for both the leukemia and RMS cells studied. To our knowledge, a number of these mechanisms are known for leukemic cells; however, to date, there are no reports on sarcoma or RMS cells. Finally, another pathway that our analysis predicted involves the interaction of the p38 kinase with the MAX TF (MYC associated factor X) known to form complexes along with other proteins for gene regulation (116). In particular, the JAK-STAT pathway is essential for embryonic stem cell renewal and proliferation (117), suggesting that it is still active in the present system.

Cell cycle. Though we have described the signaling pathways that affect cell proliferation, we have not described how these are finally implemented in the cell cycle itself. A key regulator of cell cycle progression is the MAPK pathway. Depending on the signaling of MAPK, the cell cycle pathway receives signals in order to proceed or stop its progression. In our system, it seems that key-molecules of the MAPK pathway signal down-

stream the activation of cell cycle progression. The cell cycle in these two cell types follows a time-dependent shift from the G1- to the S phase, while the G2-phase remains practically constant (Fig. 2C and D). The CCRF-CEM cell line has a defective TP53 gene (118) which appears to be unable to interact with PCNA. Also, PCNA expression is linked to the S-phase transition (119) which agrees with our result showing that PCNA is overexpressed in the leukemic cells which progress more rapidly into S-phase than the RMS cells. Interestingly, histone deacetylase 7 (HDAC7), expressed in our system, is a class II histone deacetylase, known to be tissue-specific (120). This class of histone deacetylases is an anti-apoptotic factor reported in thymocytes (121) overexpressed in the RMS cells.

Modelling JAK-STAT/MAPK and TGF-β signaling pathways. In our search for oncogenic drivers, we attempted to model the JAK-STAT-MAPK-TGF-β pathways. This analysis revealed that JAK1, STAT1, PIAS2 and CDK4 are possible gene candidates. The fact that these molecules thrive to infinitesimal oscillatory behavior, in the absence of inhibitory mechanisms, enables them to be candidate oncogenic drivers. A number of genes have already been reported as possible oncogenic drivers, such as the PRDM proteins, which belong to the SET domain family of histone methyltransferases. Enzymatic activity has been determined for only a few PRDMs suggesting that they act by recruiting co-factors or, more speculatively, confer methylation of non-histone targets. PRDM family members are deregulated in human diseases, especially in hematological malignancies and solid cancers, where they can act as both tumor suppressors and oncogenic drivers (122). Similar reports have shown the existence of such genes in glioblastoma, where a post-transcriptional regulation layer of surprising magnitude, comprising more than 248,000 microRNA-mediated interactions was revealed. Analyses in cell lines confirmed that this network regulates established drivers of tumor initiation and subtype implementation, including PTEN, PDGFRA, RB1, VEGFA, STAT3 and RUNX1, suggesting that these interactions mediate crosstalk between canonical oncogenic pathways (123). This is in agreement with our data, since we also predicted the possible role of VEGF, PDGF and STAT molecules in oncogenesis. It is also interesting that these molecules play a role in the diversity of the hematopoetic population and possibly in the leukemic populations (124). These observations bring mutations to mind. It was thought that mutations are the main driving force of tumors. However, based on the present predictions and a previous report on the so-called 'backseat drivers' (125), it is possible that mutations are not the leading or driving events in tumors. From the present predictions, it appears that there are certain molecules in a pathway that function in an unpredictable way, which can lead a system towards infinity. In other words, these molecules are capable of driving the progression of the cell cycle. Thus, a malfunction and not solely one mutation could thus be the leading event in tumorigenesis. To the best of our knowledge there are no reports referring to the non-linear nature of the gene behavior of JAK, STAT and PIAS2. However, it has been reported that the CDK family of proteins follow non-linear dynamics as potentiators of the cell cycle, and this is in agreement with our predictions. Further investigations on this topic would give us more insight on the mechanics of gene regulation and could possibly lead to the discovery of new prognostic or therapeutic targets.

In conclusion, the present study reveals a new holistic approach to understanding the dynamics of tumoral onset and possible driving forces. JAK1, STAT1, PIAS2 and CDK4 were predicted to be the driving forces in the CCRF-CEM and TE-671 cell lines. It is also suggested that mutations are not the sole driving forces behind tumorigenesis. Various neoplasms bearing different characteristics are expected to possess different traits and phenotypes. However, an approach to identify commonalities between such diverse biological systems, could possibly lead to the understanding of the common mechanisms that transform the physiological cells into malignant ones.

Acknowledgements

This study was supported in part by an independent research grant from the Financial Mechanism Office of Iceland, Liechtenstein and Norway and the Hellenic Ministry of Economy, Competitiveness and Shipping to Professor G.P. Chrousos.

References

1. Nicolis SK: Cancer stem cells and 'stemness' genes in neuro-oncology. Neurobiol Dis 25: 217-229, 2007.
2. Perilongo G, Felix CA, Meadows AT, Nowell P, Biegel J and Lange BJ: Sequential development of Wilms tumor, T-cell acute lymphoblastic leukemia, medulloblastoma and myeloid leukemia in a child with type 1 neurofibromatosis: a clinical and cytogenetic case report. Leukemia 7: 912-915, 1993.
3. Jacobs JF, Brasseur F, Hulsbergen-van de Kaa CA, *et al*: Cancer-germline gene expression in pediatric solid tumors using quantitative real-time PCR. Int J Cancer 120: 67-74, 2007.
4. Jacobs JF, Grauer OM, Brasseur F, *et al*: Selective cancer-germline gene expression in pediatric brain tumors. J Neurooncol 88: 273-280, 2008.
5. Mhawech-Fauceglia P, Herrmann FR, Bshara W, *et al*: Friend leukaemia integration-1 expression in malignant and benign tumours: a multiple tumour tissue microarray analysis using polyclonal antibody. J Clin Pathol 60: 694-700, 2007.
6. Blandford MC, Barr FG, Lynch JC, Randall RL, Qualman SJ and Keller C: Rhabdomyosarcomas utilize developmental, myogenic growth factors for disease advantage: a report from the Children's Oncology Group. Pediatr Blood Cancer 46: 329-338, 2006.
7. Chang LW, Nagarajan R, Magee JA, Milbrandt J and Stormo GD: A systematic model to predict transcriptional regulatory mechanisms based on overrepresentation of transcription factor binding profiles. Genome Res 16: 405-413, 2006.
8. Pleasance ED, Stephens PJ, O'Meara S, *et al*: A small-cell lung cancer genome with complex signatures of tobacco exposure. Nature 463: 184-190, 2009.
9. Wood LD, Parsons DW, Jones S, *et al*: The genomic landscapes of human breast and colorectal cancers. Science 318: 1108-1113, 2007.
10. Mosse YP, Laudenslager M, Longo L, *et al*: Identification of ALK as a major familial neuroblastoma predisposition gene. Nature 455: 930-935, 2008.
11. Mardis ER, Ding L, Dooling DJ, *et al*: Recurring mutations found by sequencing an acute myeloid leukemia genome. N Engl J Med 361: 1058-1066, 2009.
12. Jones S, Zhang X, Parsons DW, *et al*: Core signaling pathways in human pancreatic cancers revealed by global genomic analyses. Science 321: 1801-1806, 2008.
13. Parsons DW JS, Zhang X, *et al*: An integrated genomic analysis of human glioblastoma multiforme. Science 26: 1807-1812, 2008.
14. Sandberg AA, Stone JF, Czarnecki L and Cohen JD: Hematologic masquerade of rhabdomyosarcoma. Am J Hematol 68: 51-57, 2001.
15. Parham DM, Pinto A, Tallini G and Novak RW: Rhabdomyosarcoma mimicking acute leukemia. Arch Pathol Lab Med 122: 1047, 1998.

16. Morandi S, Manna A, Sabattini E and Porcellini A: Rhabdomyosarcoma presenting as acute leukemia. J Pediatr Hematol Oncol 18: 305-307, 1996.
17. Putti MC, Montaldi A, D'Emilio A, *et al*: Unusual leukemic presentation of rhabdomyosarcoma: report of two cases with immunological, ultrastructural and cytogenetical studies. Haematologica 76: 368-374, 1991.
18. Kaplinsky C, Frisch A, Cohen IJ, *et al*: T-cell acute lymphoblastic leukemia following therapy of rhabdomyosarcoma. Med Pediatr Oncol 20: 229-231, 1992.
19. Dedrick RL and Morrison PF: Carcinogenic potency of alkylating agents in rodents and humans. Cancer Res 52: 2464-2467, 1992.
20. Park DJ and Koeffler HP: Therapy-related myelodysplastic syndromes. Semin Hematol 33: 256-273, 1996.
21. Kelly PN, Dakic A, Adams JM, Nutt SL and Strasser A: Tumor growth need not be driven by rare cancer stem cells. Science 317: 337, 2007.
22. Khan J, Simon R, Bittner M, *et al*: Gene expression profiling of alveolar rhabdomyosarcoma with cDNA microarrays. Cancer Res 58: 5009-5013, 1998.
23. Miranda L, Wolf J, Pichuantes S, Duke R and Franzusoff A: Isolation of the human PC6 gene encoding the putative host protease for HIV-1 gp160 processing in $CD4^+$ T lymphocytes. Proc Natl Acad Sci USA 93: 7695-7700, 1996.
24. Naujokat C, Sezer O, Zinke H, Leclere A, Hauptmann S and Possinger K: Proteasome inhibitors induced caspase-dependent apoptosis and accumulation of p21WAF1/Cip1 in human immature leukemic cells. Eur J Haematol 65: 221-236, 2000.
25. Foley GE, Lazarus H, Farber S, Uzman BG, Boone BA and McCarthy RE: Continuous culture of human lymphoblasts from peripheral blood of a child with acute leukemia. Cancer 18: 522-529, 1965.
26. Uzman BG, Foley GE, Farber S and Lazarus H: Morphologic variations in human leukemic lymphoblasts (CCRF-CEM cells) after long-term culture and exposure to chemotherapeutic agents. A study with the electron microscope. Cancer 19: 1725-1742, 1966.
27. Sandstrom PA and Buttke TM: Autocrine production of extracellular catalase prevents apoptosis of the human CEM T-cell line in serum-free medium. Proc Natl Acad Sci USA 90: 4708-4712, 1993.
28. McAllister RM, Isaacs H, Rongey R, *et al*: Establishment of a human medulloblastoma cell line. Int J Cancer 20: 206-212, 1977.
29. Friedman HS, Bigner SH, McComb RD, *et al*: A model for human medulloblastoma. Growth, morphology, and chromosomal analysis in vitro and in athymic mice. J Neuropathol Exp Neurol 42: 485-503, 1983.
30. McAllister RM, Melnyk J, Finkelstein JZ, Adams EC Jr and Gardner MB: Cultivation in vitro of cells derived from a human rhabdomyosarcoma. Cancer 24: 520-526, 1969.
31. Yeung CM, An BS, Cheng CK, Chow BK and Leung PC: Expression and transcriptional regulation of the GnRH receptor gene in human neuronal cells. Mol Hum Reprod 11: 837-842, 2005.
32. Chu ES, Wong TK and Yow CM: Photodynamic effect in medulloblastoma: downregulation of matrix metalloproteinases and human telomerase reverse transcriptase expressions. Photochem Photobiol Sci 7: 76-83, 2008.
33. Ormerod MG and Payne AW: Display of three-parametric data acquired by a flow cytometer. Cytometry 8: 240-243, 1987.
34. Ormerod MG, Payne AW and Watson JV: Improved program for the analysis of DNA histograms. Cytometry 8: 637-641, 1987.
35. Watson JV, Chambers SH and Smith PJ: A pragmatic approach to the analysis of DNA histograms with a definable G1 peak. Cytometry 8: 1-8, 1987.
36. Chung HW, Park SW, Chung JB, *et al*: Differences in genetic expression profiles between young-age and old-age gastric adenocarcinoma using cDNA microarray for endocrine disruptor study. Oncol Rep 12: 33-39, 2004.
37. Chatziioannou A, Moulos P and Kolisis FN: Gene ARMADA: an integrated multi-analysis platform for microarray data implemented in MATLAB. BMC Bioinformatics 10: 354, 2009.
38. Sifakis EG, Prentza A, Koutsouris D and Chatziioannou AA: Evaluating the effect of various background correction methods regarding noise reduction, in two-channel microarray data. Comput Biol Med: Nov 8, 2011 (Epub ahead of print).
39. Zhang D, Zhang M and Wells MT: Multiplicative background correction for spotted microarrays to improve reproducibility. Genet Res 87: 195-206, 2006.
40. Tseng GC, Oh MK, Rohlin L, Liao JC and Wong WH: Issues in cDNA microarray analysis: quality filtering, channel normalization, models of variations and assessment of gene effects. Nucleic Acids Res 29: 2549-2557, 2001.
41. Hoffmann R, Seidl T and Dugas M: Profound effect of normalization on detection of differentially expressed genes in oligonucleotide microarray data analysis. Genome Biol 3: RESEARCH0033, 2002.
42. Hoffmann R, Seidl T, Bruno L and Dugas M: Developmental markers of B cells are superior to those of T cells for identification of stages with distinct gene expression profiles. J Leukoc Biol 74: 602-610, 2003.
43. Yang IV, Chen E, Hasseman JP, *et al*: Within the fold: assessing differential expression measures and reproducibility in microarray assays. Genome Biol 3: research0062, 2002.
44. Shabalin AA, Tjelmeland H, Fan C, Perou CM and Nobel AB: Merging two gene-expression studies via cross-platform normalization. Bioinformatics 24: 1154-1160, 2008.
45. Ramasamy A, Mondry A, Holmes CC and Altman DG: Key issues in conducting a meta-analysis of gene expression microarray datasets. PLoS Med 5: e184, 2008.
46. Russel S, Meadows L and Russel RR: Microarray Technology in Practice. Elsevier Inc., London, 2009.
47. Benson DA, Karsch-Mizrachi I, Lipman DJ, Ostell J and Wheeler DL: GenBank. Nucleic Acids Res 31: 23-27, 2003.
48. Benson DA, Karsch-Mizrachi I, Lipman DJ, Ostell J and Wheeler DL: GenBank: update. Nucleic Acids Res 32: D23-D26, 2004.
49. Schuler GD: Sequence mapping by electronic PCR. Genome Res 7: 541-550, 1997.
50. Wheeler DL, Church DM, Edgar R, *et al*: Database resources of the National Center for Biotechnology Information: update. Nucleic Acids Res 32: D35-40, 2004.
51. Wheeler DL, Church DM, Federhen S, *et al*: Database resources of the National Center for Biotechnology. Nucleic Acids Res 31: 28-33, 2003.
52. Diehn M, Sherlock G, Binkley G, *et al*: SOURCE: a unified genomic resource of functional annotations, ontologies, and gene expression data. Nucleic Acids Res 31: 219-223, 2003.
53. Perez-Iratxeta C, Wjst M, Bork P and Andrade MA: G2D: a tool for mining genes associated with disease. BMC Genet 6: 45, 2005.
54. Causton H, Quackenbush J and Brazma A: Microarray gene expression data analysis : A beginner's guide. Blackwell Publishing, Malden, MA, 2003.
55. Cleveland W: Robust locally weighted regression and smoothing scatterplots. Journal of the American Statistical Association 74: 829-836, 1979.
56. Klipper-Aurbach Y, Wasserman M, Braunspiegel-Weintrob N, *et al*: Mathematical formulae for the prediction of the residual beta cell function during the first two years of disease in children and adolescents with insulin-dependent diabetes mellitus. Med Hypotheses 45: 486-490, 1995.
57. Storey JD and Tibshirani R: Statistical significance for genome-wide studies. Proc Natl Acad Sci USA 100: 9440-9445, 2003.
58. Storey JD and Tibshirani R: Statistical methods for identifying differentially expressed genes in DNA microarrays. Methods Mol Biol 224: 149-157, 2003.
59. Cohen BA, Mitra RD, Hughes JD and Church GM: A computational analysis of whole-genome expression data reveals chromosomal domains of gene expression. Nat Genet 26: 183-186, 2000.
60. Sturn A, Quackenbush J and Trajanoski Z: Genesis: cluster analysis of microarray data. Bioinformatics 18: 207-208, 2002.
61. Reyal F, Stransky N, Bernard-Pierrot I, *et al*: Visualizing chromosomes as transcriptome correlation maps: evidence of chromosomal domains containing co-expressed genes - a study of 130 invasive ductal breast carcinomas. Cancer Res 65: 1376-1383, 2005.
62. Zhang B, Schmoyer D, Kirov S and Snoddy J: GOTree Machine (GOTM): a web-based platform for interpreting sets of interesting genes using Gene Ontology hierarchies. BMC Bioinformatics 5: 16, 2004.
63. Cole SW, Yan W, Galic Z, Arevalo J and Zack JA: Expression-based monitoring of transcription factor activity: the TELiS database. Bioinformatics 21: 803-810, 2005.
64. Wingender E, Dietze P, Karas H and Knuppel R: TRANSFAC: a database on transcription factors and their DNA binding sites. Nucleic Acids Res 24: 238-241, 1996.
65. Beisvag V, Junge FK, Bergum H, *et al*: GeneTools - application for functional annotation and statistical hypothesis testing. BMC Bioinformatics 7: 470, 2006.

66. Rubinstein R and Simon I: MILANO - custom annotation of microarray results using automatic literature searches. BMC Bioinformatics 6: 12, 2005.
67. Mlecnik B, Scheideler M, Hackl H, Hartler J, Sanchez-Cabo F and Trajanoski Z: PathwayExplorer: web service for visualizing high-throughput expression data on biological pathways. Nucleic Acids Res 33: W633-W637, 2005.
68. Kanehisa M: A database for post-genome analysis. Trends Genet 13: 375-376, 1997.
69. Nakao M, Bono H, Kawashima S, *et al*: Genome-scale Gene Expression Analysis and Pathway Reconstruction in KEGG. Genome Inform Ser Workshop Genome Inform 10: 94-103, 1999.
70. Kanehisa M and Goto S: KEGG: kyoto encyclopedia of genes and genomes. Nucleic Acids Res 28: 27-30, 2000.
71. Kanehisa M: The KEGG database. Novartis Found Symp 247: 91-101; discussion 101-103, 119-128, 244-252, 2002.
72. Ogata H, Goto S, Sato K, Fujibuchi W, Bono H and Kanehisa M: KEGG: Kyoto Encyclopedia of Genes and Genomes. Nucleic Acids Res 27: 29-34, 1999.
73. Funahashi A, Morohashi M, Kitano H and Tanimura N: CellDesigner: a process diagram editor for gene-regulatory and biochemical networks. BioSilico 1: 159-162, 2003.
74. Funahashi A, Matsuoka Y, Jouraku A, Morohashi M, Kikuchi N and Kitano H: CellDesigner 3.5: A Versatile Modeling Tool for Biochemical Networks. Proceedings of the IEEE 96: 1254-1265, 2008.
75. Moutselos K, Kanaris I, Chatziioannou A, Maglogiannis I and Kolisis FN: KEGGconverter: a tool for the in-silico modelling of metabolic networks of the KEGG Pathways database. BMC Bioinformatics 10: 324, 2009.
76. Brown VI, Hulitt J, Fish J, *et al*: Thymic stromal-derived lymphopoietin induces proliferation of pre-B leukemia and antagonizes mTOR inhibitors, suggesting a role for interleukin-7Ralpha signaling. Cancer Res 67: 9963-9970, 2007.
77. Barata JT, Keenan TD, Silva A, Nadler LM, Boussiotis VA and Cardoso AA: Common gamma chain-signaling cytokines promote proliferation of T-cell acute lymphoblastic leukemia. Haematologica 89: 1459-1467, 2004.
78. Kiss C, Benko I and Kovacs P: Leukemic cells and the cytokine patchwork. Pediatr Blood Cancer 42: 113-121, 2004.
79. Hiroi M and Ohmori Y: Constitutive nuclear factor kappaB activity is required to elicit interferon-gamma-induced expression of chemokine CXC ligand 9 (CXCL9) and CXCL10 in human tumour cell lines. Biochem J 376: 393-402, 2003.
80. de la Iglesia N, Konopka G, Puram SV, *et al*: Identification of a PTEN-regulated STAT3 brain tumor suppressor pathway. Genes Dev 22: 449-462, 2008.
81. Yoshino J, Monkawa T, Tsuji M, Hayashi M and Saruta T: Leukemia inhibitory factor is involved in tubular regeneration after experimental acute renal failure. J Am Soc Nephrol 14: 3090-3101, 2003.
82. Niini T, Vettenranta K, Hollmen J, *et al*: Expression of myeloid-specific genes in childhood acute lymphoblastic leukemia - a cDNA array study. Leukemia 16: 2213-2221, 2002.
83. Ho CL, Hsu LF, Phyliky RL and Li CY: Autocrine expression of platelet-derived growth factor B in B cell chronic lymphocytic leukemia. Acta Haematol 114: 133-140, 2005.
84. Karamysheva AF: Mechanisms of angiogenesis. Biochemistry (Mosc) 73: 751-762, 2008.
85. Weimar IS, Miranda N, Muller EJ, *et al*: Hepatocyte growth factor/scatter factor (HGF/SF) is produced by human bone marrow stromal cells and promotes proliferation, adhesion and survival of human hematopoietic progenitor cells ($CD34^+$). Exp Hematol 26: 885-894, 1998.
86. Choi YL, Tsukasaki K, O'Neill MC, *et al*: A genomic analysis of adult T-cell leukemia. Oncogene 26: 1245-1255, 2007.
87. Zhelyazkova AG, Tonchev AB, Kolova P, Ivanova L and Gercheva L: Prognostic significance of hepatocyte growth factor and microvessel bone marrow density in patients with chronic myeloid leukaemia. Scand J Clin Lab Invest 1-9, 2008.
88. Accordi B, Pillozzi S, Dell'Orto MC, *et al*: Hepatocyte growth factor receptor c-MET is associated with FAS and when activated enhances drug-induced apoptosis in pediatric B acute lymphoblastic leukemia with TEL-AML1 translocation. J Biol Chem 282: 29384-29393, 2007.
89. Scholl C, Gilliland DG and Frohling S: Deregulation of signaling pathways in acute myeloid leukemia. Semin Oncol 35: 336-345, 2008.
90. Hara J, Matsuda Y, Fujisaki H, *et a*l: Expression of adhesion molecules in childhood B-lineage-cell neoplasms. Int J Hematol 72: 69-73, 2000.
91. Raynaud F, Marcilhac A, Chebli K, Benyamin Y and Rossel M: Calpain 2 expression pattern and sub-cellular localization during mouse embryogenesis. Int J Dev Biol 52: 383-388, 2008.
92. Grovdal LM, Johannessen LE, Rodland MS, Madshus IH and Stang E: Dysregulation of Ack1 inhibits down-regulation of the EGF receptor. Exp Cell Res 314: 1292-1300, 2008.
93. Shen F, Lin Q, Gu Y, Childress C and Yang W: Activated Cdc42-associated kinase 1 is a component of EGF receptor signaling complex and regulates EGF receptor degradation. Mol Biol Cell 18: 732-742, 2007.
94. Mamali I, Kotsantis P, Lampropoulou M and Marmaras VJ: Elk-1 associates with FAK, regulates the expression of FAK and MAP kinases as well as apoptosis in HK-2 cells. J Cell Physiol 216: 198-206, 2008.
95. Rogers RS, Horvath CM and Matunis MJ: SUMO modification of STAT1 and its role in PIAS-mediated inhibition of gene activation. J Biol Chem 278: 30091-30097, 2003.
96. Kisseleva T, Bhattacharya S, Braunstein J and Schindler CW: Signaling through the JAK/STAT pathway, recent advances and future challenges. Gene 285: 1-24, 2002.
97. Levy DE and Darnell JE Jr: Stats: transcriptional control and biological impact. Nat Rev Mol Cell Biol 3: 651-662, 2002.
98. Korzus E, Torchia J, Rose DW, *et al*: Transcription factor-specific requirements for coactivators and their acetyltransferase functions. Science 279: 703-707, 1998.
99. Hiroi M and Ohmori Y: The transcriptional coactivator CREB-binding protein cooperates with STAT1 and NF-kappa B for synergistic transcriptional activation of the CXC ligand 9/monokine induced by interferon-gamma gene. J Biol Chem 278: 651-660, 2003.
100. So EY, Oh J, Jang JY, Kim JH and Lee CE: Ras/Erk pathway positively regulates Jak1/STAT6 activity and IL-4 gene expression in Jurkat T cells. Mol Immunol 44: 3416-3426, 2007.
101. Dorsey JF, Cunnick JM, Mane SM and Wu J: Regulation of the Erk2-Elk1 signaling pathway and megakaryocytic differentiation of Bcr-Abl(+) K562 leukemic cells by Gab2. Blood 99: 1388-1397, 2002.
102. Delaunoy J, Abidi F, Zeniou M, *et al*: Mutations in the X-linked RSK2 gene (RPS6KA3) in patients with Coffin-Lowry syndrome. Hum Mutat 17: 103-116, 2001.
103. Yang SH, Shore P, Willingham N, Lakey JH and Sharrocks AD: The mechanism of phosphorylation-inducible activation of the ETS-domain transcription factor Elk-1. EMBO J 18: 5666-5674, 1999.
104. Sharrocks AD: The ETS-domain transcription factor family. Nat Rev Mol Cell Biol 2: 827-837, 2001.
105. Shaw PE and Saxton J: Ternary complex factors: prime nuclear targets for mitogen-activated protein kinases. Int J Biochem Cell Biol 35: 1210-1226, 2003.
106. Zhang HM, Li L, Papadopoulou N, *et al*: Mitogen-induced recruitment of ERK and MSK to SRE promoter complexes by ternary complex factor Elk-1. Nucleic Acids Res 36: 2594-2607, 2008.
107. Ohshima T and Shimotohno K: Transforming growth factor-beta-mediated signaling via the p38 MAP kinase pathway activates Smad-dependent transcription through SUMO-1 modification of Smad4. J Biol Chem 278: 50833-50842, 2003.
108. Hu PP, Shen X, Huang D, Liu Y, Counter C and Wang XF: The MEK pathway is required for stimulation of p21(WAF1/CIP1) by transforming growth factor-beta. J Biol Chem 274: 35381-35387, 1999.
109. Yue J and Mulder KM: Requirement of Ras/MAPK pathway activation by transforming growth factor beta for transforming growth factor beta 1 production in a smad-dependent pathway. J Biol Chem 275: 35656, 2000.
110. Engel ME, McDonnell MA, Law BK and Moses HL: Interdependent SMAD and JNK signaling in transforming growth factor-beta-mediated transcription. J Biol Chem 274: 37413-37420, 1999.
111. Hocevar BA, Brown TL and Howe PH: TGF-beta induces fibronectin synthesis through a c-Jun N-terminal kinase-dependent, Smad4-independent pathway. EMBO J 18: 1345-1356, 1999.
112. Raingeaud J, Gupta S, Rogers JS, *et al*: Pro-inflammatory cytokines and environmental stress cause p38 mitogen-activated protein kinase activation by dual phosphorylation on tyrosine and threonine. J Biol Chem 270: 7420-7426, 1995.
113. Raingeaud J, Whitmarsh AJ, Barrett T, Derijard B and Davis RJ: MKK3- and MKK6-regulated gene expression is mediated by the p38 mitogen-activated protein kinase signal transduction pathway. Mol Cell Biol 16: 1247-1255, 1996.

114. Whitmarsh AJ, Yang SH, Su MS, Sharrocks AD and Davis RJ: Role of p38 and JNK mitogen-activated protein kinases in the activation of ternary complex factors. Mol Cell Biol 17: 2360-2371, 1997.
115. Price MA, Cruzalegui FH and Treisman R: The p38 and ERK MAP kinase pathways cooperate to activate Ternary Complex Factors and c-fos transcription in response to UV light. EMBO J 15: 6552-6563, 1996.
116. Lee CM, Onesime D, Reddy CD, Dhanasekaran N and Reddy EP: JLP: A scaffolding protein that tethers JNK/p38MAPK signaling modules and transcription factors. Proc Natl Acad Sci USA 99: 14189-14194, 2002.
117. Rho JY, Yu K, Han JS, *et al*: Transcriptional profiling of the developmentally important signalling pathways in human embryonic stem cells. Hum Reprod 21: 405-412, 2006.
118. Strasser-Wozak EM, Hartmann BL, Geley S, *et al*: Irradiation induces G2/M cell cycle arrest and apoptosis in p53-deficient lymphoblastic leukemia cells without affecting Bcl-2 and Bax expression. Cell Death Differ 5: 687-693, 1998.
119. Tonkinson JL, Marder P, Andis SL, *et al*: Cell cycle effects of antifolate antimetabolites: implications for cytotoxicity and cytostasis. Cancer Chemother Pharmacol 39: 521-531, 1997.
120. Verdin E, Dequiedt F and Kasler HG: Class II histone deacetylases: versatile regulators. Trends Genet 19: 286-293, 2003.
121. Dequiedt F, Kasler H, Fischle W, *et al*: HDAC7, a thymus-specific class II histone deacetylase, regulates Nur77 transcription and TCR-mediated apoptosis. Immunity 18: 687-698, 2003.
122. Fog CK, Galli GG and Lund AH: PRDM proteins: Important players in differentiation and disease. Bioessays 34: 50-60, 2012.
123. Sumazin P, Yang X, Chiu HS, *et al*: An extensive microRNA-mediated network of RNA-RNA interactions regulates established oncogenic pathways in glioblastoma. Cell 147: 370-381, 2011.
124. Hoang T: The origin of hematopoietic cell type diversity. Oncogene 23: 7188-7198, 2004.
125. Futreal PA: Backseat drivers take the wheel. Cancer Cell 12: 493-494, 2007.